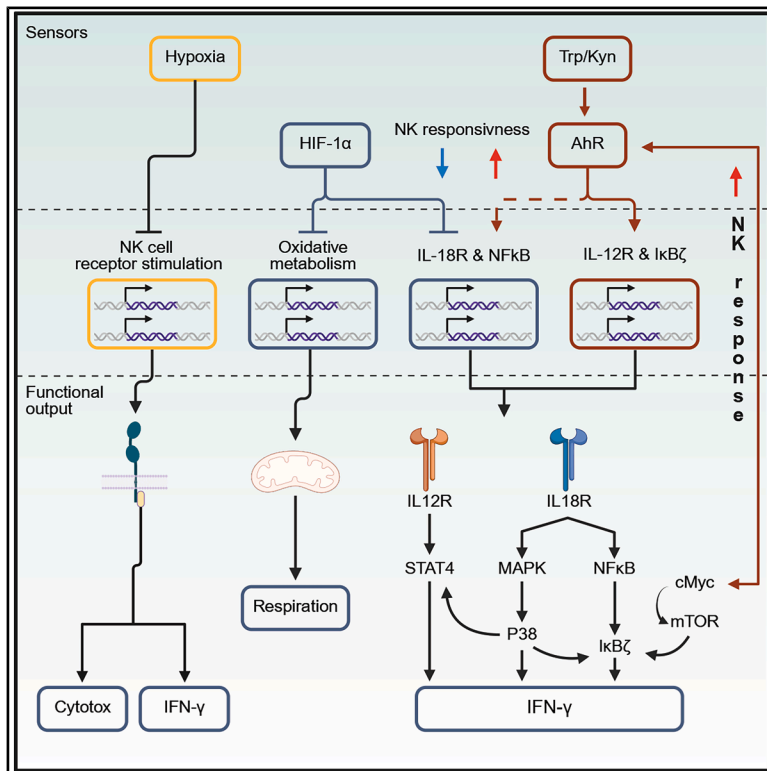


Functional segregation of HIF-1 α and AhR controls NK cell responsiveness under hypoxia

Graphical abstract



Authors

Sebastiano Giorgetta,
 Francesco Cortopassi,
 Theodoros Chanis, ..., Michael Platten,
 Adelheid Cerwenka, Ana Stojanovic

Correspondence

ana.stojanovic@medma.uni-heidelberg.de

In brief

Biological sciences; Molecular biology;
 Immunology

Highlights

- AhR and HIF-1 α regulate NK cell effector outputs in hypoxia
- Hypoxia transcriptionally represses OxPhos and the IL-12R/18R pathway via HIF-1 α
- AhR activation preserves IL-12/18-induced IFN- γ production in hypoxia
- AhR opposes HIF-1 α -mediated suppression by engaging the cMyc-mTORC1-I κ B ζ pathway



Article

Functional segregation of HIF-1 α and AhR controls NK cell responsiveness under hypoxia

Sebastiano Giorgetta,^{1,2,11} Francesco Cortopassi,^{1,2,11} Theodoros Chanis,^{1,2} Jing Ni,^{1,2} Margareta P. Correia,^{1,2,3} Carsten Sticht,⁴ Volker Ast,^{4,5} Michael Platten,^{2,6,7,8,9} Adelheid Cerwenka,^{1,2,9,10,12} and Ana Stojanovic^{1,2,12,13,*}

¹Department of Immunobiochemistry, Medical Faculty Mannheim, Heidelberg University, Mannheim, Germany

²Mannheim Institute for Innate Immunoscience (MI3), Medical Faculty Mannheim, Heidelberg University, Mannheim, Germany

³Cancer Biology and Epigenetics Group, Research Center of IPO Porto (CI-IPOP)/RISE@CI-IPOP, Portuguese Oncology Institute of Porto (IPO-Porto, Porto), Porto, Portugal

⁴NGS Core Facility, Medical Faculty Mannheim, Heidelberg University, Mannheim, Germany

⁵Institute for Clinical Chemistry, University Medicine Mannheim (UMM), Mannheim, Germany

⁶German Cancer Consortium (DKTK), Heidelberg, Germany

⁷German Cancer Research Center (DKFZ), CCU Neuroimmunology and Brain Tumor Immunology, Heidelberg, Germany

⁸Department of Neurology, Medical Faculty Mannheim, Center for Translational Neuroscience (MCTN), Heidelberg University, Mannheim, Germany

⁹DKFZ Hector Cancer Institute at the University Medical Center Mannheim, Mannheim, Germany

¹⁰European Center for Angioscience (ECAS), Medical Faculty Mannheim, Heidelberg University, Mannheim, Germany

¹¹These authors contributed equally

¹²These authors contributed equally

¹³Lead contact

*Correspondence: ana.stojanovic@medma.uni-heidelberg.de

<https://doi.org/10.1016/j.isci.2026.115492>

SUMMARY

Multiple mechanisms operate to transform microenvironmental information into cellular adaptation, but how environmental sensors mechanistically synergize to fine-tune natural killer (NK) cell functions is underexplored. Although the deletion of HIF-1 α , the sensor for hypoxia, was shown to impact NK cell responses, we here demonstrate that hypoxia-inflicted adaptations in NK cells are differentially hard-wired through HIF-1 α . The hypoxia-HIF-1 α axis repressed NK cell oxidative metabolism and the response to IL-12/18 through transcription. However, the IL-12/18-induced IFN- γ production was preserved under hypoxia. This was attributed to the activation of the aryl-hydrocarbon receptor (AhR) that magnified the engagement of the cMyc-mTORC1-I κ B ζ pathway, resulting in elevated IFN- γ expression. NK cells harmonized AhR/HIF-1 α -mediated signals through defined transcriptional modules, also detected in similar microenvironments, such as in solid tumors. Together, NK cell functions are fine-tuned through regulatory networks controlled by environmental sensors, which act as superordinate checkpoints for NK cell outputs.

INTRODUCTION

The primary function of natural killer (NK) cells is the recognition and elimination of stressed, infected, and malignant cells. This process relies on the arrays of the receptors expressed on the cell surface that deliver signals for cytotoxic function.¹ In addition, both soluble mediators and surface receptors can trigger NK cells to produce cytokines² and assume auxiliary roles in immune response. NK cell responsiveness toward pathological threats is also determined by environmental cues sensed at the cellular level. Both healthy and inflamed tissues are characterized by sets of determinants that affect immune responses, such as nutrient availability, tissue stiffness, oxygen tension or acidity (pH).^{3–6} NK cells were shown to respond to these signals by adapting their functional outputs.^{7–10} However, how different signals derived from target cells and the environment are

processed together, and how the different NK cell functions are altered according to the received inputs, is not fully explored.

Tissues present a distinctive physiological concentration of oxygen available to parenchymal and accessory tissue cells.¹¹ In pathological conditions, such as inflammation or cancer, available oxygen is scarce, leading to hypoxia.^{12,13} Cellular adaptations to hypoxia are facilitated by hypoxia-sensitive transcription factors (TFs), including HIF-1 α (hypoxia inducible factor 1 subunit alpha), which alter gene and protein expression to amend to the newly met metabolic demands of the cell.¹⁴ Hypoxia was shown to alter functions of immune effector cells, including NK cells^{10,15} and CD8⁺ T cells.^{16,17} HIF-1 α was reported to regulate NK cell IFN- γ production in hypoxia, as well as NK cell anti-tumor,^{8,18} anti-viral,¹⁹ and anti-bacterial responses.²⁰ However, the relative contribution of HIF-1 α to hypoxia-inflicted functional changes is not entirely clear.



To perform its functions, HIF-1 α interacts with numerous proteins and transcriptional regulators,²¹ and can affect gene expression both directly and indirectly. Transcriptional activity of HIF-1 α is tied to dimerization with ARNT (HIF-1 β), which results in a conformational change crucial for high-affinity DNA binding of the complex.²² On the other hand, CBP/p300 acts as a HIF-1 α coactivator by increasing its acetylation and, thus its transcriptional activity.²³ Both ARNT and CBP/p300 can also form a transcriptional complex with a ligand-activated TF aryl-hydrocarbon receptor (AhR).²⁴ AhR was initially identified for its role in metabolizing xenobiotics and regulating the expression of cytochrome P450 enzymes.²⁵ However, multiple studies demonstrated its role in many physiological functions, including immune cell regulation.²⁶ Physiological ligands that can activate AhR in these settings include tryptophan derivatives, such as kynurenine,^{27,28} as well as some dietary and microbial-derived compounds.^{29,30} AhR has been shown to regulate mouse NK cell IFN- γ production, cytotoxicity,³¹ and migration,³² as well as human NK cell development^{33,34} and the expression of activating surface receptors.³⁵ Due to shared interaction partners, the functions of AhR and HIF-1 α are closely associated.³⁶ Here, we show that NK cells harmonize AhR- and HIF-1 α -derived signals through segregated transcriptional modules, enabling stimuli-dependent regulation of NK cell effector responses. Hypoxia and HIF-1 α regulated oxidative metabolism and the response to cytokines IL-12/18 through transcription. Despite transcriptional repression, the activation of AhR enabled the preservation of IFN- γ production under hypoxia, by enhancing the expression of IL-12R chains and Nfkbiz (I κ B ζ), and by engaging the cMyc-mTORC1-I κ B ζ pathway downstream of IL-12 and IL-18 receptor activation. Therefore, we propose that at the concurrence of hypoxia and propinquity of tryptophan or its metabolites, AhR can act as a salvage checkpoint to maintain proinflammatory NK cell output.

RESULTS

Hypoxia regulates metabolism- and function-associated NK cell transcriptome

To investigate how NK cells adapt their functions when exposed to hypoxia for prolonged time periods, we cultured mouse splenic NK cells in normoxia (20% O₂) or hypoxia (1% O₂) for 7 days, and analyzed their transcriptomes. NK cells derived from these cultures displayed a differential abundance of transcripts that encode proteins involved in metabolism and NK cell effector responses (Figure 1A). Hypoxia inflicted the transcriptional repression of oxidative respiration, while increasing glycolysis (Figures 1A and 1B), and regulated pathways related to the activation of various NK cell receptors (Figure 1C, left). Pathways operating via CD3 ζ (Cd247), Syk/Zap70 (Syk, Lcp2/SLP76), PI3K (Pik3cd/p110 δ), and Vav (Vav2) were suppressed in hypoxia, indicating a repression of ITAM-mediated responses. In addition, we detected a lower abundance of transcripts affecting the MAPK pathway and activation of NF- κ B (Nfkb1, Nfkb2, Nfkbia, Nfkbib, Nfkbie, Rela, Relb), which support NK cell activation by cytokines, such as IL-18³⁷⁻³⁹ (Figure 1C, right). Suppression of this pathway was further supported by higher amounts of Irak3, encoding for a negative regulator of MyD88-dependent

signaling.⁴⁰ In contrast, the amount of Il12rb2 (IL-12R β 2) was higher in NK cells under hypoxia. These data indicate that hypoxia transcriptionally directs not only metabolic adaptation to low oxygen concentration, but also has broad effects on the pathways that conduct NK cell effector outputs.

Hypoxia-HIF-1 α -reliant regulation of NK cell IFN- γ production is stimulus-dependent

To determine if transcriptional changes inflicted by exposure to hypoxia resulted in the altered function of NK cells, we assessed metabolic output, cytotoxicity, and production of IFN- γ by NK cells cultured in normoxia or hypoxia. NK cells cultured in hypoxia manifested reduced basal and maximal oxygen consumption rates (Figure 2A). Alongside, we detected a reduced proportion of both RMA-S (MHC class I-deficient) and RMA-Rae1 γ (NKG2D-ligand overexpressing) tumor cells displaying caspase 3/7 activation in co-culture with NK cells derived from hypoxic cultures (Figure 2B), indicating the effect of hypoxia on both missing-self and NKG2D-mediated cytotoxicity. Similarly, when stimulated via the activating receptor NK1.1 that engages the Syk/Zap70 kinase pathway,^{41,42} lower proportions of NK cells cultured in hypoxia produced IFN- γ compared to normoxia-derived controls (Figure 2C). However, hypoxia did not affect either the frequency of cells producing IFN- γ or the amount of cytokine produced if NK cells were stimulated with IL-12 and IL-18 (IL-12/18) (Figure 2D), despite the transcriptional repression of the pathway downstream of the IL-12 and IL-18 receptors (IL-12R/18R) (Figure 1C, right). These data evidence that the transcriptional regulation of oxidative metabolism and activating receptor-affiliated pathways mirrors reduced NK cell function under hypoxia. However, despite transcriptional repression, NK cells cultured in hypoxia preserved the response to IL-12/18.

To identify and predict the activity of TFs regulating adaptation to hypoxia, we performed TF inference analysis,⁴³ which predicted low activity of proinflammatory programs driven by NF- κ B and IRF TFs, while regulatory factors, such as Erg, were predicted as active (Figure 3A). Our data also predicted the activation of HIF-1 α , which is stabilized in hypoxia and often referred to as a master regulator of cellular adaptation to low oxygen tension.¹⁴ HIF-1 α likely coordinated changes in gene expression in cooperation with other factors, resulting in modified cellular functions.

To determine how the divergent functional responses of NK cells under hypoxia are affected by HIF-1 α , we cultured control or Hif1a-deficient NK cells, derived from mice with a conditional Hif1a deficiency in Ncr1-expressing cells (Ncr1^{iCre} Hif1a^{fl/fl}),⁸ under hypoxia, and determined their functional output. Compared to controls, Hif1a-deficient NK cells displayed an increased basal and maximal oxygen consumption rate (Figure 3B). These data corresponded to changes in the transcriptome detected between control and Hif1a-deficient NK cells cultured under hypoxia, with the latter displaying higher abundance of transcripts related to oxidative phosphorylation, concomitant with an overall reduction of transcripts related to glycolysis (Figure S1B). Transcripts related to activating receptor signaling were differentially affected by the absence of HIF-1 α . Syk, Lcp2 (SLP76), and Vav2 were more abundant, indicating their transcriptional regulation via the hypoxia-HIF-1 α axis. However, the amounts of cytotoxic effector molecule mRNAs Gzmb and

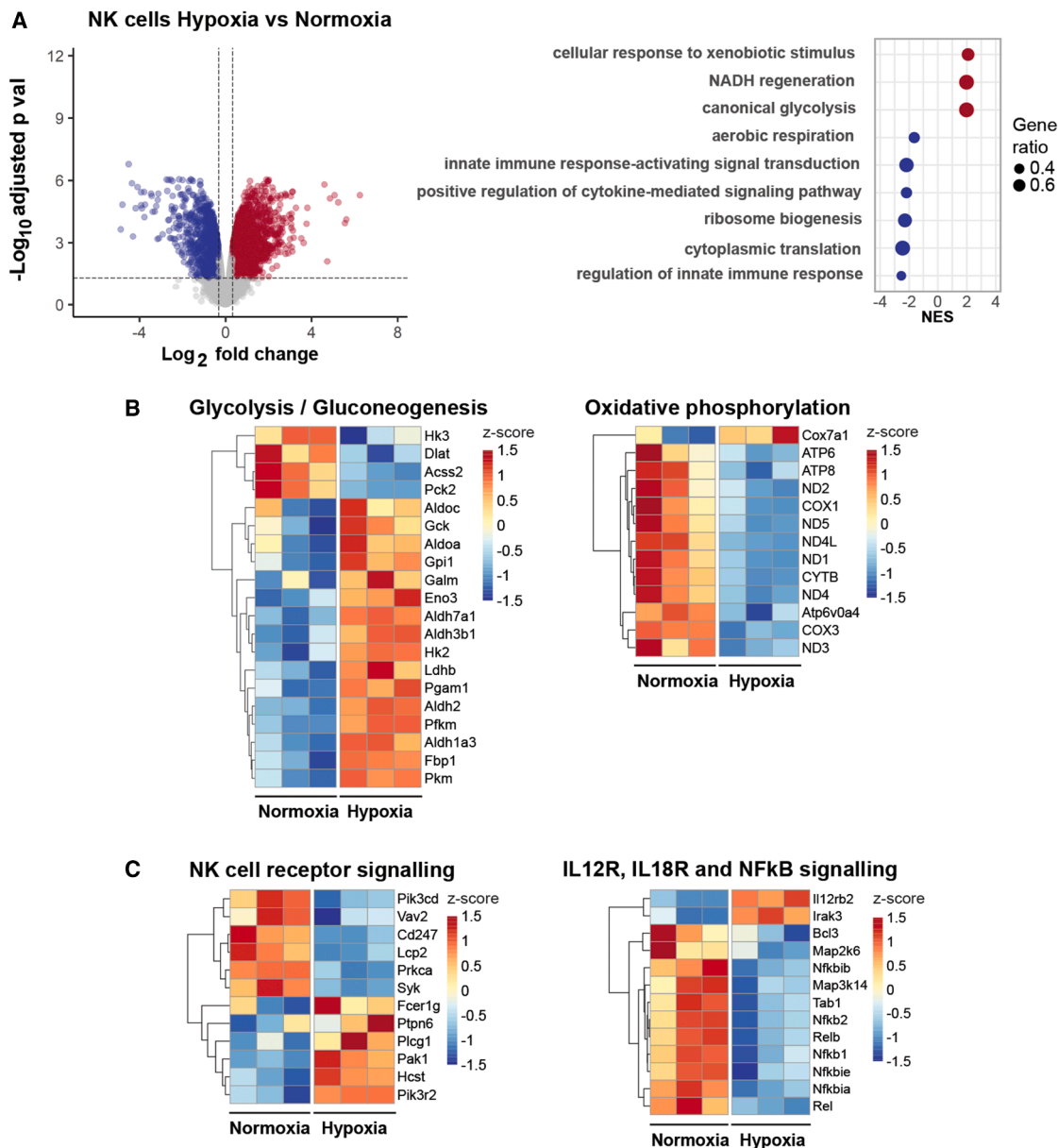


Figure 1. Hypoxia regulates metabolism and function-associated NK cell transcriptome

Mouse splenic NK cells were cultured in normoxia or hypoxia for 7 days, and then subjected to mRNA-sequencing.

(A) Volcano plot (left) indicates differential abundance of transcripts in NK cells cultured in hypoxia compared to NK cells derived from control cultures (normoxia). Red – increased, blue – decreased transcript abundance (fold change > |1.25|, p-adjusted <0.05). Dot plot (right) indicates selected GO Biological Processes affected by differentially abundant transcripts (NES, normalized enrichment score).

(B and C) Heatmaps show differentially abundant transcripts associated with metabolism (B), and response to activating receptor-triggering or stimulation with the cytokines IL-12 and IL-18 (C).

Prf1 were reduced (Figure S1B). Consequent to this differential regulation, NK cell cytotoxicity assessed via caspase 3/7 activation in tumor cells did not differ between control and Hif1a-deficient NK cells (Figure 3C).

Next, we assessed IFN- γ production triggered via the activating receptor NK1.1 or via IL-12R/IL-18R. Alike cytotoxicity, IFN- γ production triggered via NK1.1-engagement was not affected (Figure 3D). In contrast, a higher proportion of NK cells

made IFN- γ in the absence of HIF-1 α (Figure 3E) when stimulated with IL12/18. In concert, Hif1a-deficient NK cells presented higher amounts of transcripts encoding for IL-12R, IL-18R, and several members of the NF- κ B signaling pathway (Figure S1B).

Together, our data show that activating receptor-mediated responses, including both cytotoxicity and IFN- γ production, were affected by hypoxia, but did not increase in the context of Hif1a deficiency, indicating that several, but not all, hypoxia-inflicted

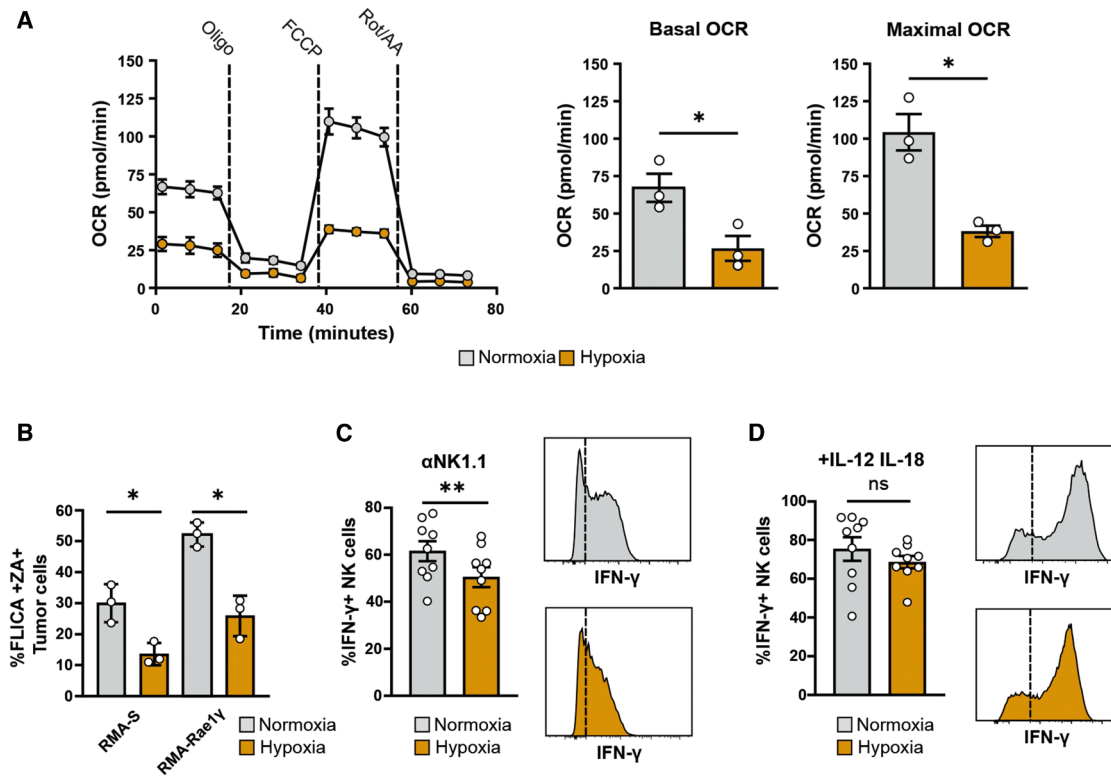


Figure 2. Hypoxia-reliant regulation of NK cell IFN- γ production is stimulus-dependent

Mouse splenic NK cells were cultured in normoxia or hypoxia for 7 days.

(A) Oxygen consumption rate (OCR) was measured upon the addition of Oligomycin (Oligo), Carbonyl cyanide 4-(trifluoromethoxy)phenylhydrazone (FCCP), and rotenone/antimycin A (Rot/AA) at the indicated time points. Data represent OCR over time (left), or basal and maximal OCR (right), as mean \pm SEM, $n = 3$, $*p \leq 0.05$ by paired t test.

(B) NK cells were incubated with tumor cells for 5h. FLICA reagent for the detection of caspase 3/7 activity was added for the last hour of the co-culture. Zombie Aqua (ZA) reagent was used to label apoptotic cells. Frequency of apoptotic tumor cells with activated caspases was determined by flow cytometry. Data represent mean \pm SEM, $n = 3$, $*p \leq 0.05$ by paired t test.

(C and D) NK cells were stimulated with plate-bound α NK1.1 mAb (C) or with IL-12 and IL-18 (D) for 5h. Frequencies of IFN- γ -producing NK cells were determined by flow cytometry (left). Representative histogram plots of IFN- γ expression are shown (right). Data represent mean \pm SEM, $n = 9$, $**p \leq 0.01$ or not significant (ns) by paired t test.

changes within these pathways were mediated solely by HIF-1 α . Indeed, the intersection of our two datasets, comparing the transcripts affected by hypoxia (hypoxia vs. normoxia) with the transcripts affected by HIF-1 α under hypoxia (Hif1a-deficient vs. control NK cells), suggests that approximately half of the transcripts under hypoxia were directly or indirectly regulated by HIF-1 α (Figure S1A). The hypoxia-HIF-1 α -axis regulated NK cell oxidative metabolism and response to IL-12 and IL-18 through transcription. However, as IFN- γ production induced by IL-12/IL-18 was preserved under hypoxia and further boosted in the absence of HIF-1 α , we hypothesized the existence of a mechanism that acts to maintain IFN- γ production in response to IL-12/IL-18, despite hypoxia-HIF-1 α -driven transcriptional repression of this pathway.

AhR activation elevates NK cell IFN- γ production via the cMyc-mTORC1 pathway

Among the pathways active in NK cells under hypoxia, xenobiotic metabolism (Figure 1A, right) was among the most enriched,

indicative of activation of the ligand-induced TF AhR.²⁶ In cell culture, AhR can be activated by endogenous ligands, which are derived from metabolism of the amino acid tryptophan.^{44,45} Under hypoxia, NK cells displayed higher expression of AhR mRNA and its target genes, including the canonical targets Tiparp and Cyp1b1,^{46,47} as well as Nfkb1 and Relb^{48,49} (Figure S2A). To investigate the effects of AhR on NK cell effector responses, we cultured NK cells from mice bearing conditional AhR deficiency in Ncr1-expressing cells in tryptophan-free medium, and added kynurenine, a degradation product of tryptophan, to activate AhR.⁴⁵ AhR activation did not impact IFN- γ production in response to NK1.1-triggering (Figure S2E). However, in response to IL-12/18, the frequencies of cells producing IFN- γ , and the amount of IFN- γ produced, increased when AhR-sufficient NK cells were cultured in the presence of kynurenine (Figure 4A). The selective effect of AhR on the IL-12R/18R pathway in NK cells was in agreement with data obtained by the transcriptome analysis of AhR-sufficient and AhR-deficient NK cells cultured in hypoxia for 7 days. Dataset intersection with hypoxia-affected

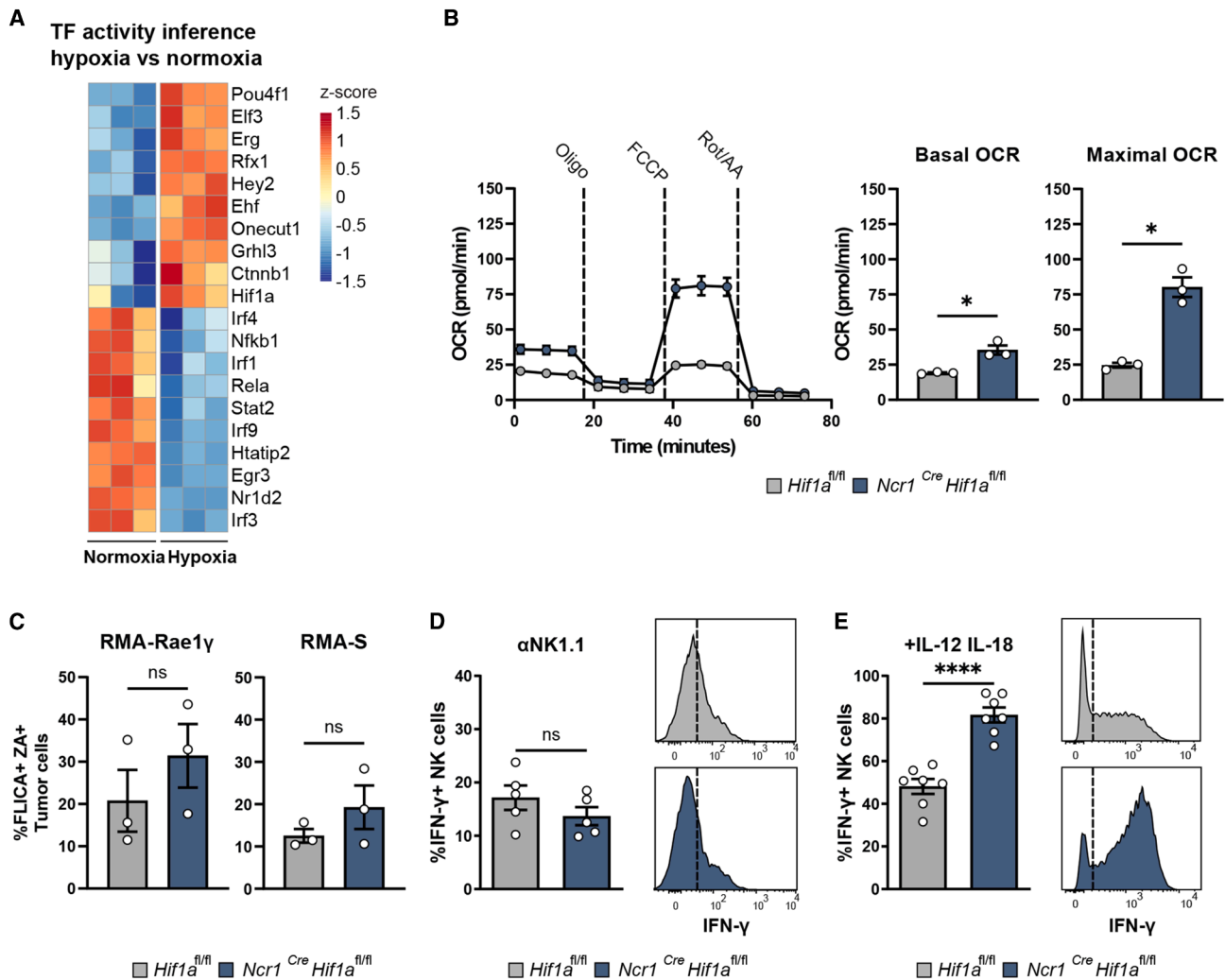


Figure 3. HIF-1 α suppresses oxidative metabolism and IFN- γ production in response to IL-12/18 under hypoxia

(A) Mouse splenic NK cells were cultured in normoxia or hypoxia for 7 days and then subjected to mRNA-sequencing. Heatmap shows the top 10 more or less active transcription factor (TF) modules predicted based on differential abundance of transcripts. (B–E) NK cells were isolated from control $Hif1a^{fl/fl}$ or $Ncr1^{Cre}Hif1a^{fl/fl}$ mice and cultured in hypoxia for 7 days. (B) Oxygen consumption rate (OCR) was measured upon the addition of oligomycin (Oligo), carbonyl cyanide 4-(trifluoromethoxy)phenylhydrazone (FCCP), and Rotenone/Antimycin A (Rot/AA) at the indicated time points. Data represent OCR over time (left), or basal and maximal OCR (right), as mean \pm SEM, $n = 3$ individual animals (2 male, 1 female), * $p \leq 0.05$ by unpaired t test. (C) NK cells were incubated with tumor cells for 5h at a 1:1 ratio for 5h. FLICA reagent for the detection of caspase 3/7 activity was added for the last hour of the co-culture. Zombie Aqua (ZA) reagent was used to label apoptotic cells. Frequency of apoptotic tumor cells with activated caspases was determined by flow cytometry. Data represent mean \pm SEM, $n = 3$, not significant (ns) by unpaired t test. (D–E) NK cells were stimulated with plate-bound α NK1.1 mAb (D) or IL-12 and IL-18 (E) for 5h. IFN- γ expression was determined by flow cytometry. Data represent mean \pm SEM, $n = 5$ (D), $n = 7$ (E), **** $p \leq 0.0001$ or not significant (ns) by unpaired t test. See also Figure S1.

transcripts denoted that a quarter of these transcripts were directly or indirectly regulated by AhR (Figure S2B). Among these, only a limited number of transcripts related to metabolism and activating receptor signaling were differentially detected in AhR-deficient compared to control NK cells (Figure S2C). However, AhR-deficient NK cells showed consistently reduced numbers of transcripts encoding IL-12R and IL-18R chains, as well as of $I\kappa B\zeta$, a nuclear coactivator in the NF- κ B pathway shown to directly regulate the transcription of the *Irfng* gene in NK cells⁵⁰ (Figure S2C). Correspondently, we detected reduced protein expression of IL-18R α in AhR-deficient, but not in $Hif1a$ -deficient

NK cells, compared to their respective controls (Figure S2F). These data indicate that pre-exposure to AhR-ligands could set up the threshold for response to IL-12/18 by transcriptionally regulating the expression of their receptors.

We have previously shown that, apart from the mobilization of NF- κ B, the stimulation of NK cells via IL-18R also led to the activation of the mammalian target of rapamycin complex 1 (mTORC1), along with an upregulation of cMyc and $I\kappa B\zeta$ expression.⁹ Indeed, IL-12R/18R-triggering induced the phosphorylation of the ribosomal protein S6 (pS6) in a higher proportion of NK cells compared to the activation of the NK1.1 receptor

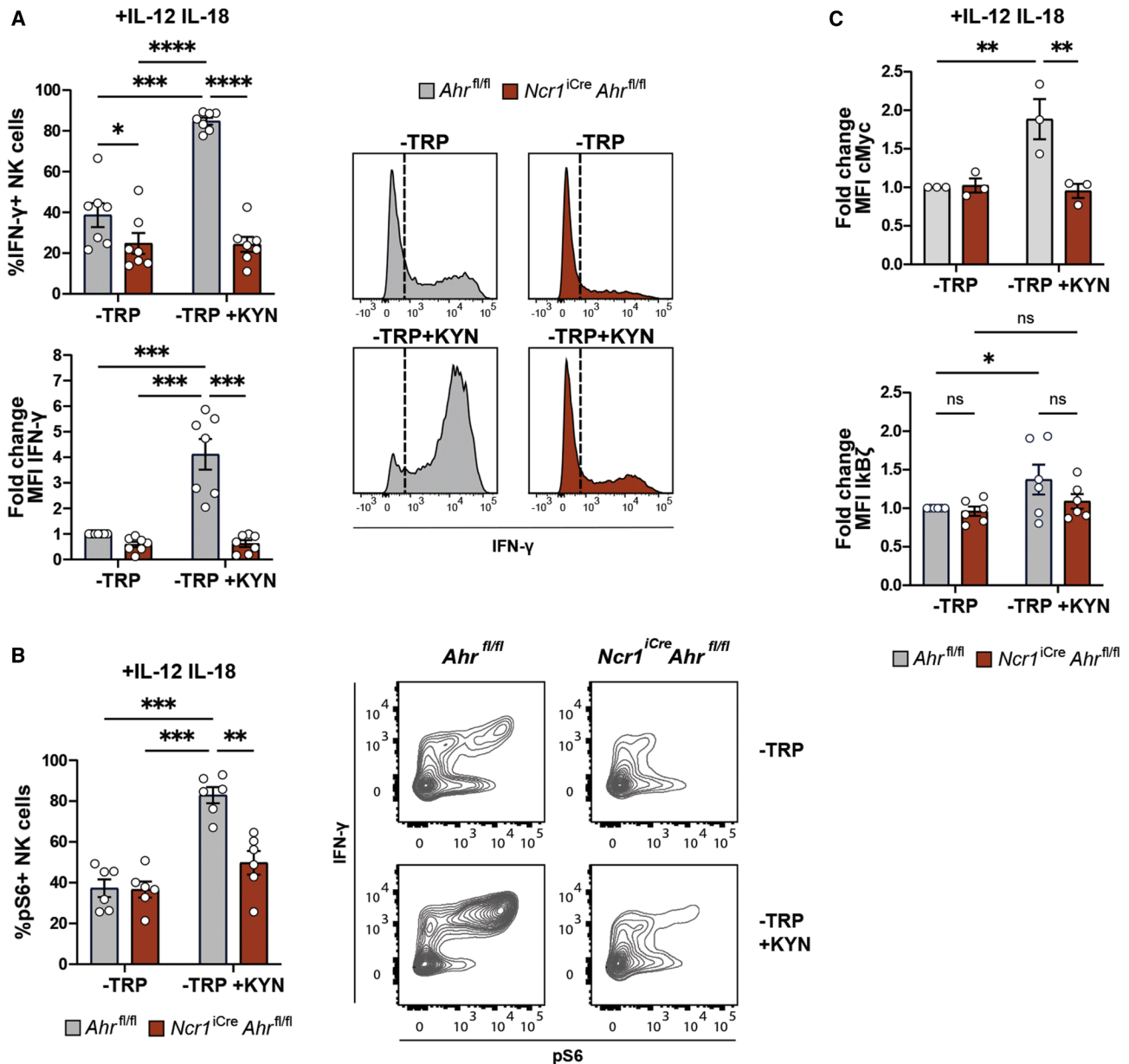


Figure 4. AhR activation elevates NK cell IFN- γ production via cMyc-mTORC1 pathway

(A–C) Splenic NK cells were isolated from Rag2-deficient control (*Ahr*^{fl/fl}) or *Ncr1*^{iCre} *Ahr*^{fl/fl} mice, and cultured in tryptophan-free media (-TRP) supplemented with kynurenine (-TRP+KYN) for 7 days. NK cells were stimulated with IL-12 and IL-18 for 5h. Expression of IFN- γ (A), phosphorylated-S6 (pS6) (B), cMyc, and I κ B ζ (C) was determined by flow cytometry. Representative histogram plots of IFN- γ expression (A), and contour plots of IFN- γ and pS6 co-expression (B) in NK cells are shown. Fold-change of IFN- γ , cMyc, and I κ B ζ expression relative to the expression in control *Ahr*^{fl/fl} NK cells cultured in tryptophan-free media was calculated for every independent experiment. Data represent mean \pm SEM, $n = 7$ (A), $n = 6$ (B), $n = 3$, (C, up), $n = 6$ (C, down); ** $p \leq 0.01$, *** $p \leq 0.001$, and **** $p \leq 0.0001$ by two-way ANOVA corrected for multiple comparison (Tukey) (A, up; B). * $p \leq 0.05$ by ratio t test with the false discovery rate (FDR) for multiple comparison correction (A, down; C). MFI, mean fluorescence intensity. See also Figures S2 and S3.

(Figure S3A), and led to increased cMyc and I κ B ζ expression (Figure S3B). To investigate if AhR affected NK cell response to IL-12/18 via mTORC1, cMyc, and/or I κ B ζ , we assessed pS6, cMyc, and/or I κ B ζ expression in AhR-sufficient and deficient NK cells exposed to IL-12/18. AhR-sufficient NK cells exposed to kynurenine displayed higher mTORC1 activation (measured by pS6 expression) when stimulated with IL-12/18 (Figure 4B,

left), which correlated with higher IFN- γ expression (Figure 4B, right). Concomitantly, the expression of cMyc and I κ B ζ increased in AhR-sufficient compared to AhR-deficient NK cells when cultured in the presence of kynurenine (Figure 4C). The importance of mTORC1 to initiate cMyc upregulation in IL-12/18-stimulated NK cells was previously reported,⁵¹ while I κ B ζ was shown to bind to the Irfng promoter and promote Irfng

mRNA transcription.^{50,52} To explore if mTORC1, cMyc, and IκBζ act as a sequential circuit downstream of AhR activation to support IFN-γ production, we utilized Torin2 (mTORC1 inhibitor) and 10058-F4 (inhibitor of cMyc:Max dimerization), and measured IFN-γ, pS6, cMyc, and IκBζ expression upon NK cell stimulation with IL-12 and IL-18. The inhibitors marginally affected proportions of NK cells producing IFN-γ, but abrogated the kynurenine-mediated increase of the amount of IFN-γ produced by NK cells (Figure S3C). Further, Torin2 prevented the increase of IκBζ expression by IL-12/18 in kynurenine-treated NK cells, indicating that mTORC1 acted downstream of AhR activation and upstream of IκBζ (Figure S3D). In the presence of the 10058-F4 inhibitor, no mTORC1 activation was detected (Figure S3D), suggesting that cMyc operates upstream of mTORC1. Our analysis suggested that AhR likely does not affect mTORC1 activation through the transcriptome (Figure S2D). However, some cMyc target gene products were downregulated in AhR-deficient compared to control NK cells (Figure S2D), suggesting that cMyc expression might be affected by AhR, independent of stimulation with IL-12/18.

Together, AhR exerts both transcriptional and non-transcriptional executive roles in regulating the responsiveness of NK cells to IL-12/18 and the amount of IFN-γ produced, respectively. AhR governs the transcription of IκBζ and IL-12R/18R-chains mRNAs, assuring the higher responsiveness to stimulation. Upon stimulation, AhR magnifies the engagement of cMyc-mTORC1-IκBζ pathway, leading to elevated IFN-γ expression.

Deletion of Hif1a leads to an AhR-dependent boost of IL-12/18-induced IFN-γ production under hypoxia

Our data show that the absence of Ahr resulted in a lower number of transcripts encoding IκBζ, IL-12R, and IL-18R chains (Figure S2), thereby opposing the effect of HIF-1α (Figure 1C). Hence, we postulated that AhR activation could be a mechanism that acts to maintain IFN-γ production in response to IL-12/IL-18, despite hypoxia-HIF-1α-driven transcriptional repression. To test this, we have generated mice with conditional deficiency of both Hif1a and Ahr in Ncr1-expressing cells (Ncr1^{Cre} Hif1a^{fl/fl} Ahr^{fl/fl}).

The frequencies of IFN-γ-producing Hif1a/Ahr-deficient NK cells cultured under hypoxia did not increase upon stimulation with IL-12/18, as observed for Hif1a-deficient NK cells (Figure 5A). Alongside, no increase in the frequency of pS6-expressing cells (Figure 5B), or cMyc (Figure 5C) and IκBζ expression (Figure 5D) was observed in IL-12/18-stimulated Hif1a/Ahr-deficient NK cells, indicating that the cMyc-mTORC1-IκBζ pathway could not be engaged in the context of Hif1a-deficiency when AhR is absent, and therefore, no boost of IFN-γ production can be enforced. Moreover, culture of Hif1a-deficient NK cells in tryptophan-free medium phenocopied the response to IL-12/18 of Hif1a/Ahr-deficient NK cells (Figure S4A), further verifying that AhR activation was necessary to boost IFN-γ production in the context of Hif1a deficiency. In contrast, the absence of Ahr in the context of Hif1a deficiency altered neither NK cell oxygen consumption rates (Figure 5E), nor IFN-γ production in response to NK1.1-triggering (Figure S4B).

NK cells display HIF-1α and AhR regulatory modules in hypoxia and in solid tumor tissue of mouse and human

Our data show that the interplay of microenvironmental factors via their cellular sensors can fine-tune NK cell responses, leading to the selective suppression or activation of their effector responses. Our transcriptome analyses of Hif1a- and Ahr-deficient NK cells indicated the existence of HIF-1α and AhR “regulatory modules” that shape the NK cell transcriptome, and thereby their functions. Thus, we aimed at determining common and/or discrete HIF-1α and AhR “regulatory modules” by comparing single (Hif1a or Ahr)-deficient and double (Ahr and Hif1a)-deficient NK cell transcriptomes. We cultured NK cells under hypoxia in tryptophan-sufficient medium to stabilize HIF-1α and permit AhR activation and thus HIF-1α- and AhR-dependent gene transcription. Differentially abundant transcripts grouped into up- or downregulated modules driven by the respective NK cell genotypes (Figure 6A). The data show that within these modules, either AhR or HIF-1α exerted dominant regulatory roles, which suggested that these pathways segregate to regulate transcription in NK cells under hypoxia. The AhR module encompassed genes/transcripts that were differentially regulated whenever NK cells lacked Ahr, namely in both Ahr-deficient and Ahr/Hif1a double-deficient NK cells. These included the previously reported Ahr-regulated/target genes *Il12rb1* and *Kit*^{29,54,55} as a part of the AhR-up module (regulated by AhR, reduced when NK cells are Ahr-deficient), while the HIF-1α-up module comprised its reported targets *Aldoa* and *Ldha*⁵⁶ (Figure 6B). Biological processes regulated by AhR-up module transcripts included immune cell activation and signal transduction, while HIF-1α-up module affected metabolism and cellular energy (Figure S5C), consistent with its role in regulating NK cell metabolism under hypoxia (Figures S5A and S5B).

When considering the IL-12R/18R pathway, we have observed that HIF-1α exerted a dominant role in transcriptional repression (HIF-1α down module) of genes encoding STAT4 (IL-12R signaling⁵⁷), IL-18R chains, and NF-κB family, which remained reduced in the absence of Hif1a, even when AhR was active (Hif1a-deficient NK cells) (Figure 6C). A set of transcripts, including *Nfkbia*, *Nfkbib*, *Stat3*, *Jun*, *Irak2*, and *Map3k1*, was also regulated by HIF-1α independently of AhR (HIF-1α up module). In contrast, transcripts encoding IL-12R chains, JAK2 (IL-12R signaling⁵⁸), IκBζ, and MAP2K4 kinase, which activates p38,⁵⁹ were suppressed by HIF-1α and upregulated in the presence of AhR (HIF-1α down AhR up module). In these settings, p38 can support IL-18-, IL-12R/STAT4- and STAT1-mediated IFN-γ production^{60–62} and can activate the TFs NF-κB and AP-1, thereby supporting *Irfng* transcription.^{63,64} Together, our data indicate opposing functions of HIF-1α and AhR on these sets of genes, balancing their expression in a situation where both factors are active.

As we defined these divergent transcriptional roles of AhR and HIF-1α, converging into IFN-γ production in response to IL-12/18, we aimed at testing how AhR and HIF-1α operate these pathways under conditions when NK cells are exposed to both hypoxia and AhR-ligands. In solid tumors, the activation of HIF-1α was shown to hamper the ability of NK cells to control tumor growth.^{8,18} It was also reported that the tryptophan-degradation product kynurenine accumulated in tumor tissues of patients

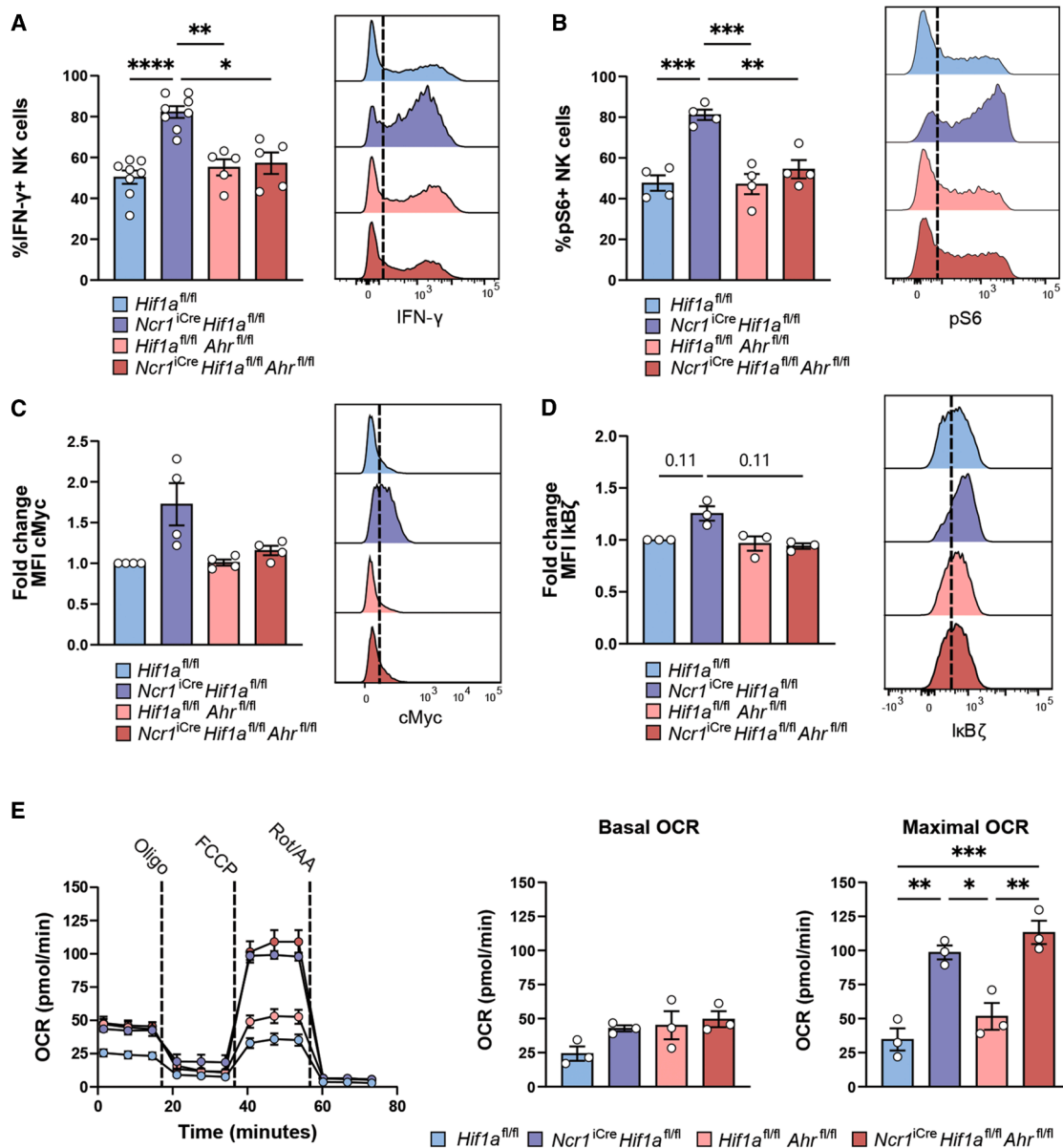


Figure 5. Deletion of Hif1a leads to an AhR-dependent boost of IL-12/18-induced IFN-γ production under hypoxia

Splenic NK cells were isolated from control *Hif1a*^{fl/fl}, *Hif1a*^{fl/fl} *Ahr*^{fl/fl} or from *Ncr1*^{iCre} *Hif1a*^{fl/fl} and *Ncr1*^{iCre} *Hif1a*^{fl/fl} *Ahr*^{fl/fl} mice, and cultured in hypoxia for 7 days. (A–D) NK cells were stimulated with IL-12 and IL-18 for 5h. Expression of IFN-γ (A), phosphorylated-S6 (pS6) (B), cMyc (C), and IκBζ (D) was determined by flow cytometry. Fold-change of cMyc and IκBζ expression relative to the expression in *Hif1a*^{fl/fl} NK cells was calculated for every independent experiment. Representative histogram plots of the expression of indicated proteins in NK cells are shown. Data represent mean ± SEM, n = 5–8 (A), n = 4 (B, C), n = 3 (D), *p ≤ 0.05, **p ≤ 0.01, ***p ≤ 0.001, and ****p ≤ 0.0001 by ordinary one-way ANOVA test corrected for multiple comparison (Tukey) (A–B); ratio t test with the false discovery rate (FDR) for multiple comparison correction (C–D).

(E) Oxygen consumption rate (OCR) was measured upon the addition of oligomycin (Oligo), carbonyl cyanide 4-(trifluoromethoxy)phenylhydrazone (FCCP), and rotenone/antimycin A (Rot/AA) at the indicated time points. Data represent OCR over time (left), basal and maximal OCR (right) as mean ± SEM, n = 3, *p ≤ 0.05, **p ≤ 0.01, and ***p ≤ 0.001 by ordinary one-way ANOVA test corrected for multiple comparison (Tukey). See also Figure S4.

with cancer.^{65,66} Therefore, we postulated that these modules could operate in solid tumor-infiltrating NK cells, creating an activation-repression balance, as observed *in vitro*. To this end, we leveraged published datasets analyzing tumor-infiltrating NK cells in mouse⁸ and human.⁵³ The data indicated that, alike *in vitro*, in mouse subcutaneous lymphoma, HIF-1α regulated

NK cell metabolism, as the set of transcripts that was downregulated in context of Hif1a deficiency in hypoxia *in vitro* was also less enriched in Hif1a-deficient tumor-infiltrating NK cells compared to controls (Figure S6A). Similarly, a set of HIF-1α-suppressed transcripts related to IL-12R/18R activation (Figure 6C) was enriched in Hif1a-deficient tumor-infiltrating

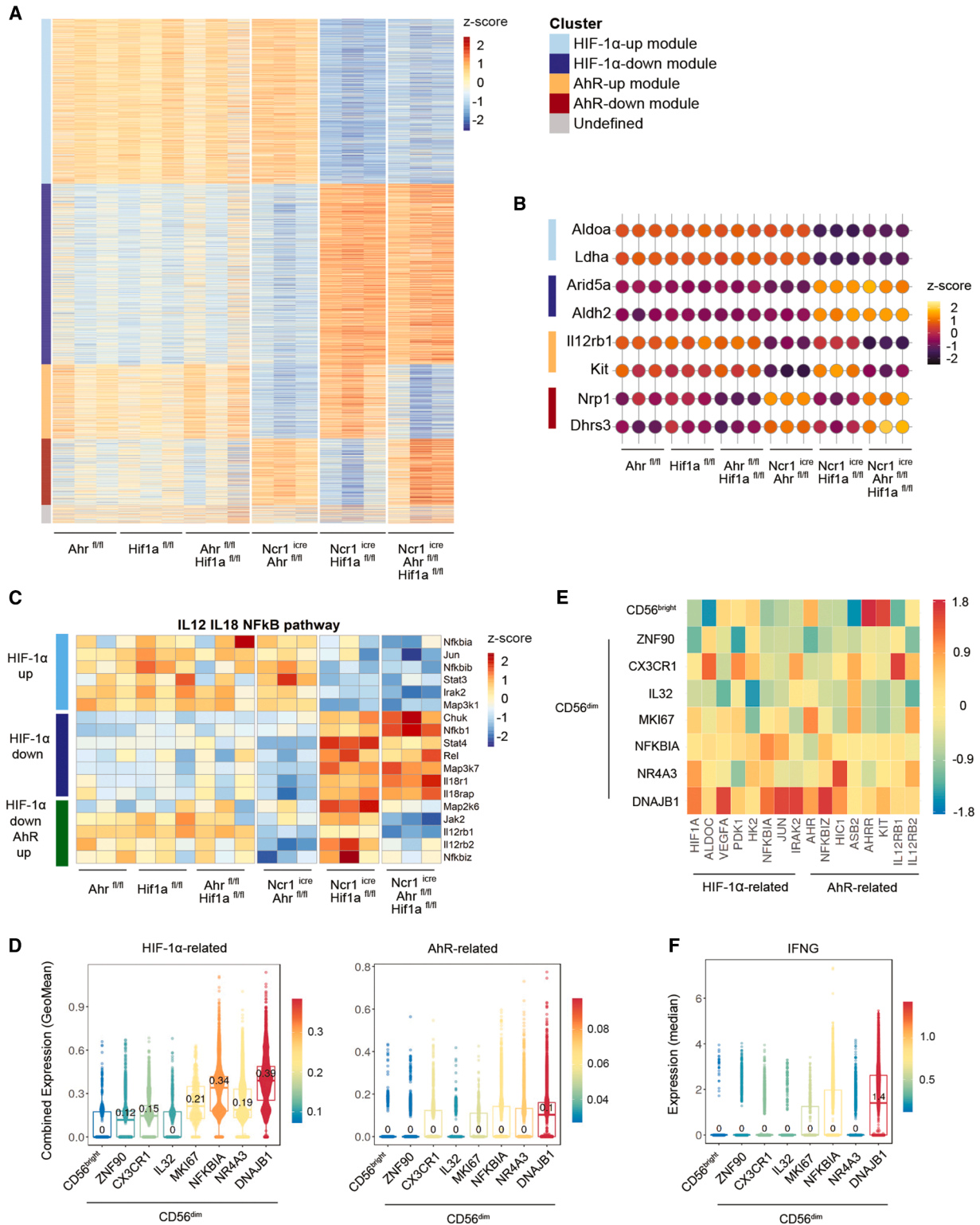


Figure 6. HIF-1α and AhR regulatory modules in hypoxia and in solid tumor tissue of mouse and human

(A and B) Splenic NK cells from control Ahr^{fl/fl}, Hif1a^{fl/fl}, Ahr^{fl/fl} Hif1a^{fl/fl}, or from Ncr1^{icre} Ahr^{fl/fl}, Ncr1^{icre} Hif1a^{fl/fl}, and Ncr1^{icre} Ahr^{fl/fl} Hif1a^{fl/fl} mice were cultured for 7 days under hypoxia, and their transcriptome was analyzed by sequencing of mRNA. (A) Heatmap shows differentially abundant transcripts (fold change >1.25), p-adjusted <0.05) detected in at least one comparison. A transcript set is considered a regulatory module if uniformly expressed among control NK cells and

(legend continued on next page)

NK cells compared to controls (Figure S6A). Enrichment of the transcripts related to AhR activation (Table S2) did not differ between Hif1a-sufficient and deficient tumor-infiltrating NK cells, consistent with a regulatory segregation of HIF-1 α and AhR. Nevertheless, the “HIF-1 α down AhR up” module was enriched in tumor-infiltrating NK cells when HIF-1 α -mediated suppression was not present (Figure S6A), consistent with our observations *in vitro* (Figure 6C).

To determine if HIF-1 α and AhR activation can be inferred in human tumor-infiltrating NK cells, we selected transcripts related to their activation (Table S2). The expression of HIF1A, AHR, and selected candidates differed in NK cells derived from various tumor types (Figure S6B). However, when analyzing tumor NK cell subsets originally defined by Tang et al.,⁵³ the enrichment scores for both HIF-1 α and AhR activation were highest in NK cells displaying cellular stress-related signatures (DNAJB1), which were postulated to have spent the longest time in the tumor tissue (Figures 6D and 6E). The DNAJB1-subset not only showed the highest expression of the transcripts related to HIF-1 α and AhR activity, but also the highest amount of IFNG (Figure 6F), suggesting that, despite being exposed to hypoxia and stress, NK cells retained the ability to produce IFN- γ . Together, these data indicate that in the context of the tumor microenvironment, both HIF-1 α and AhR sense their environmental triggers and could regulate NK cell functionality.

DISCUSSION

NK cells are early responders to infection and transformation. Particularly in the context of cancer, NK cells are considered as major antigen- and MHC class I-independent immune effectors that can be targeted and harnessed for therapy.⁶⁷ NK cell responses require cell activation through sets of surface receptors able to sense cellular stress and tissue and immune alarmins, such as inflammatory cytokines. Like other innate immune cells, NK cells can be activated via multiple germline-encoded cell surface receptors.⁶⁸ These include NK activating receptors, whose ligands are typically expressed by stressed, infected, or transformed cells, allowing their recognition and elimination, and cytokine receptors, that sense the alerts from the surrounding cells. The activation of NK cells is a product of signal integration and results in cytotoxicity (target cell killing), and/or the production of soluble mediators, of which IFN- γ is considered a “signature cytokine” produced by NK cells.^{69–71} However, both the NK cell ability to respond and the magnitude of their responses can be affected by a multitude of signals deriving from their immediate environment. How these signals interplay and how they regulate NK cell responses at the molecular level is rather underexplored.

The aptitude for NK cell activation in tissue can be dictated by various tissue attributes, including available nutrients^{51,72,73} or

physical and chemical conditions, such as the concentration of oxygen.^{8,18} Several approaches have been undertaken to increase NK cell functions in unfavourable conditions. For example, IL-15 provided to CAR-expressing NK cells increased their metabolic fitness and *in vivo* persistence in pre-clinical settings.⁷⁴ However, NK cells were eventually outcompeted by the outgrowing tumor, suggesting that their cell-intrinsic regulatory networks succumbed to the “environmental pressure,” and that rewiring these operative systems might be beneficial to provide pro-fitness signals.

Both human and mouse NK cells are affected by hypoxia.^{8,15,18,75,76} Here, we show that hypoxia restrains oxidative metabolism and the responses of NK cells mediated via activating receptors, including both cytotoxicity and cytokine production. These functional outputs are likely conjured from the transcriptional regulation, as the transcripts encoding the proteins involved in both metabolic- and activating receptor-associated functions were reduced in NK cells exposed to hypoxia. HIF-1 α mediated only a fraction of the observed NK cell adaptations to hypoxia, having the most significant effect on NK cell metabolism. Hif1a-deficient NK cells showed higher oxygen consumption under hypoxia, but did not increase responses to NK1.1-triggering, compared to controls. This can be explained by the mobilization of other hypoxia-responsive pathways in NK cells, of which we detected the plausible activation of several regulatory networks. These data indicate that under hypoxia, different transcriptional modules might be engaged to uphold the governance over differential effector assemblies of NK cells.

In contrast to activating receptor-mediated outputs, under hypoxia, NK cells preserved IFN- γ production induced by cytokine receptors for IL-12 and IL-18. Cytotoxicity is crucial for the rapid elimination of infected or transformed cells early in the immune response, while IFN- γ has broader immunoregulatory effects, including increasing antigen presentation,⁷⁷ macrophage activation,⁷⁸ and T cell differentiation.^{79,80} In addition, cytotoxicity can be rapidly triggered and quickly inhibited when controlled at the level of granule release,⁶⁹ while IFN- γ production involves multiple levels of control, including epigenetic regulation, transcription, mRNA stability, and protein synthesis.^{62,71,81–83} Preserving its production in the context of hypoxia could therefore allow a broader impact of NK cells on overall immune activation through crosstalk with other immune cells.

Our data show that the unremitting responsiveness to IL-12/18 is attained through convoluted transcriptional and post-transcriptional regulation. NK cells utilized sensing of tryptophan and its derivatives by the ligand-activated TF AhR to surpass HIF-1 α -mediated suppression. Hypoxia/HIF-1 α hindered IL-12/18-induced IFN- γ production via transcriptional suppression of the IL-18R and NF- κ B pathway. Despite the opposing effects of AhR, the inhibitory effect of HIF-1 α appears dominant.

differs in at least one group of NK cells with gene deficiency. (B) Examples of transcripts assigned to depicted modules across NK cells with different genotypes are shown.

(C) Differentially abundant transcripts from “IL12 IL18 NF κ B pathway” assigned to depicted regulatory modules.

(D–F) Relative abundance of transcripts related to HIF-1 α and AhR activation (Table S2), or IFNG (F) in human tumor-infiltrating NK cell subsets.⁵³ Boxplots depict combined enrichment scores (D) or median expression (F), and a heatmap (E) shows scaled expression for the individual transcripts. Data are generated using the pan-NK cancer atlas (<http://pan-nk.cancer-pku.cn>). See also Figure S5.

Instead, positive effects of AhR at the transcriptome level were mainly inflicted on the expression of IL-12R, I κ B ζ , and p38-activating kinase. IL-12 was reported to enhance IL-18R expression,^{84,85} while p38 can assist NF- κ B-mediated I κ B ζ transcription,⁶³ thus together counteracting HIF-1 α -mediated effects.

While the aforementioned AhR-mediated effects acted via transcriptome and preceded activation, thus setting the thresholds for NK cells' responsiveness to IL-12/18, AhR also exerted transcriptome-independent regulation that manifested upon the engagement of the IL-12R/18R. NK cells exposed to AhR-ligands were able to more efficiently engage the cMyc-mTORC1 pathway in response to IL-12/18. mTORC1 and cMyc activity in NK cells were closely linked to IL-15R signaling, which is crucial for NK cell differentiation and homeostasis.^{86–89} However, they also regulate NK cell metabolic reprogramming, whereby glucose uptake and glycolysis rates increase to sustain NK cell effector functions.^{90,91} mTORC1 promotes protein synthesis through its targets 4E-BP1 and S6K1,⁹² and the expression of nutrient transporters.^{88,90} Both mTORC1 and cMyc were shown to support the expression of the amino acid transporter SLC7A5, while in turn, SLC7A5-mediated leucine influx contributes to mTORC1 activation.^{51,72} In T cells, SLC7A5 was shown to mediate kynurenine uptake,⁹³ advocating for the connection between mTORC1, cMyc, and AhR. Although the AhR-mTORC1 axis has been suggested to operate within malignant cells,^{94,95} how AhR primes NK cells for enhanced cMyc-mTORC1 activation remains to be determined.

We have shown that stimulation with IL-12/18 also induced the expression of I κ B ζ , a nuclear coactivator in the NF- κ B pathway shown to directly regulate the transcription of the I κ B gene in NK cells.^{50,52,96} The upregulation of I κ B ζ depended on AhR, and its transcript expression was also reduced in unstimulated AhR-deficient NK cells. Inhibitors targeting mTORC1 and cMyc prevented the IL-12/18-mediated upregulation of I κ B ζ , suggesting convergence of AhR-cMyc-mTORC1 axis to I κ B ζ . I κ B ζ expression is typically induced downstream of receptors engaging the NF- κ B pathway.^{97,98} Both mTORC1 and cMyc were shown to contribute to NF- κ B-dependent survival pathways in cells.^{99,100} In addition, they both converge in regulating translation, which could affect the amount of I κ B ζ protein.

The factors that the direct activation of HIF-1 α and AhR, namely—hypoxia and AhR-ligands, can coincide in various organs, such as gut^{101,102} or liver,^{103,104} even in physiological conditions. Liver is enriched in tryptophan and its derivatives,¹⁰⁵ while AhR-ligands in gut originate from dietary sources, and from both microbial and host metabolism.¹⁰⁶ During the course of infection, oxygen concentration can drop further,⁵ while tryptophan is used by activated immune cells, leading to kynurenine accumulation.¹⁰⁷ During infection, IL-12 and IL-18 play important roles in NK cell activation and host protection.^{108,109} Therefore, we predict that in these conditions, HIF-1 α and AhR could use the proposed modular segregation to regulate NK cell functions. Hypoxia and accumulation of kynurenine are also readily reported features of solid malignancies.^{13,66,110} The depletion of tryptophan and accumulation of kynurenine were reported as detrimental for T cells, favoring the differentiation of regulatory phenotypes.^{111,112} We have detected the expression of transcripts related to IL-12R/18R activation regulated by HIF-1 α

and AhR in both mouse and human tumor-infiltrating NK cells. The data indicate that NK cells displaying stress-related signatures, which were postulated to infiltrate tumor tissue the earliest,⁵³ and therefore were exposed to the tumor microenvironment the longest, have enriched signatures for AhR- and HIF-1 α -mediated regulation of IL-12R/18R pathway. Interestingly, these cells also showed the highest abundance of IFNG transcript in the original publication by Tang et al.⁵³ Similarly, the signatures repressed by HIF-1 α were enriched in mouse Hif1a-deficient NK cell infiltrating lymphomas. We have previously shown that Hif1a-deficient NK cells were able to control the growth of these tumors,⁸ and therefore, therapeutic targeting of HIF-1 α in NK cells holds promise for enhanced anti-tumor responses. Our data, however, indicate that rather than suppressed, the AhR pathway shall be reinforced in NK cells. While AhR exerts rather inhibitory roles in the adaptive immunity,¹¹³ directly and indirectly, acting via dendritic cells,^{28,114} it was rather reported to stimulate NK cells.^{31,32} Therefore, the therapeutic application of AhR inhibitors¹¹⁵ shall be carefully considered in the context of NK cell-sensitive tumors or combinatorial therapies with NK cell therapeutics.

Together, we suggest that the segregation of the HIF-1 α and AhR pathways, and the potentially quaint AhR function in NK cells, represent a corporate solution to prevail over the allied impact of diverse inhibitory environmental conditions.

Limitations of the study

In this study, we identified a role of the TF AhR in regulating IFN- γ production by NK cells stimulated with inflammatory cytokines IL-12 and IL-18. Although not confirmed by protein detection, increased expression of AhR and its activity under hypoxia was inferred from the upregulation of its reported target genes. The role of AhR in sustaining NK cell IFN- γ production under hypoxia was associated with its capacity to boost IFN- γ production in the absence of HIF-1 α . This effect correlated with increased mTORC1 activity and elevated expression of cMyc and I κ B ζ . While these responses were AhR-dependent, the precise mechanisms by which AhR engages mTORC1 and how it contributes to cMyc, I κ B ζ , and IFN- γ expression in these settings require further investigation.

RESOURCE AVAILABILITY

Lead contact

Requests for further information and resources should be directed to and will be fulfilled by the lead contact, Dr. Ana Stojanovic (ana.stojanovic@medma.uni-heidelberg.de).

Materials availability

This study did not generate new, unique reagents. Mouse lines generated in this study are available from the [lead contact](#) with a completed materials transfer agreement.

Data and code availability

- RNA sequencing data generated in this study have been deposited in the Gene Expression Omnibus (GEO) under accession number GSE292263 and GSE292264.
- This paper does not report original code.
- This paper analyses existing, publicly available data, accessible at GEO: GSE123534 and at <http://pan-nk.cancer-pku.cn>.

- Any additional information required to reanalyze the data reported in this paper is available from the [lead contact](#) upon request.

ACKNOWLEDGMENTS

We thank Petra Bugert, Dalyan Devran, Marian Wincher, Alessia Triassi, and Patrick Matei for technical support; the animal facilities of the Medical Faculty Mannheim and the German Cancer Research Center for assistance with animal care and experiments. We thank Dagmar Gotthardt from the University of Veterinary Medicine, Vienna, for providing the Cre-expressing animal line. We gratefully acknowledge the data storage service SDS@hd supported by the Ministry of Science, Research and the Arts Baden-Württemberg (MWK) and the German Research Foundation (DFG) through grant INST 35/1503-1 FUGG. The project was supported by grants from the German Research Foundation (RTG2727 – 445549683 Innate Immune checkpoints in cancer and tissue damage [B1.2 to A.C. and A.S., B1.1 to M.P.]; SFB1366 [project number 319 394046768-SFB 1366: C02 to A.C., C01 to M.P.]; SPP1937 [CE 140/2-2 to A.S. and A.C.]; TRR179 [TP07 to A.C.]; SFB-TRR156 [B10N to A.C.]), by the German Cancer Aid translational oncology program “NK fit against AML” (74114180) (to A.C.) and by FCT (CEECINST/00091/2018) and R&D FCT (2022.04809.PTDC) grants (to M.P.C.). For the publication fee, we acknowledge financial support by Heidelberg University. Graphical abstract was created using [BioRender.com](#).

AUTHOR CONTRIBUTIONS

S.G. performed experiments related to omics, analyzed the data, and prepared figures. F.C. performed *in vitro* cell stimulation and flow cytometry. S.G. and T.C. performed experiments for revision and prepared revised figures. C.S. and S.G. analyzed bulk RNA-sequencing data. V.A. and A.S. analyzed single-cell RNA sequencing data. M.P. provided mice for the generation of conditional knock-out strains and critical input on AhR biology. M.P.C. provided input in study design and supported discussion and experiments. A.S. wrote the manuscript. A.C. and A.S. designed and supervised the study.

DECLARATION OF INTERESTS

The authors declare no competing interests.

STAR★METHODS

Detailed methods are provided in the online version of this paper and include the following:

- [KEY RESOURCES TABLE](#)
- [EXPERIMENTAL MODEL AND STUDY PARTICIPANT DETAILS](#)
 - Mice
 - Cell lines
- [METHOD DETAILS](#)
 - NK cell isolation and culture
 - NK cell stimulation
 - Flow cytometry
 - Assessment of NK cell cytotoxicity
 - Analysis of NK cell metabolism
 - RNA isolation, sequencing and data analysis
 - Analysis of mouse and human single-cell transcriptome data
- [QUANTIFICATION AND STATISTICAL ANALYSIS](#)

SUPPLEMENTAL INFORMATION

Supplemental information can be found online at <https://doi.org/10.1016/j.isci.2026.115492>.

Received: August 18, 2025
Revised: December 9, 2025
Accepted: March 24, 2026
Published: March 27, 2026

REFERENCES

1. Lanier, L.L. (2024). Five decades of natural killer cell discovery. *J. Exp. Med.* 227, e20231222. <https://doi.org/10.1084/jem.20231222>.
2. Vivier, E., Tomasello, E., Baratin, M., Walzer, T., and Ugolini, S. (2008). Functions of natural killer cells. *Nat. Immunol.* 9, 503–510. <https://doi.org/10.1038/ni1582>.
3. Xia, L., Oyang, L., Lin, J., Tan, S., Han, Y., Wu, N., Yi, P., Tang, L., Pan, Q., Rao, S., et al. (2021). The cancer metabolic reprogramming and immune response. *Mol. Cancer* 20, 28. <https://doi.org/10.1186/s12943-021-01316-8>.
4. Mai, Z., Lin, Y., Lin, P., Zhao, X., and Cui, L. (2024). Modulating extracellular matrix stiffness: a strategic approach to boost cancer immunotherapy. *Cell Death Dis.* 15, 307. <https://doi.org/10.1038/s41419-024-06697-4>.
5. Taylor, C.T., and Colgan, S.P. (2017). Regulation of immunity and inflammation by hypoxia in immunological niches. *Nat. Rev. Immunol.* 17, 774–785. <https://doi.org/10.1038/nri.2017.103>.
6. Hajjar, S., and Zhou, X. (2023). pH sensing at the intersection of tissue homeostasis and inflammation. *Trends Immunol.* 44, 807–825. <https://doi.org/10.1016/j.it.2023.08.008>.
7. Bunting, M.D., Vyas, M., Requesens, M., Langenbucher, A., Schiferle, E.B., Manguso, R.T., Lawrence, M.S., and Demehri, S. (2022). Extracellular matrix proteins regulate NK cell function in peripheral tissues. *Sci. Adv.* 8, eabk3327. <https://doi.org/10.1126/sciadv.abk3327>.
8. Ni, J., Wang, X., Stojanovic, A., Zhang, Q., Wincher, M., Bühler, L., Arnold, A., Correia, M.P., Winkler, M., Koch, P.S., et al. (2020). Single-Cell RNA Sequencing of Tumor-Infiltrating NK Cells Reveals that Inhibition of Transcription Factor HIF-1 α Unleashes NK Cell Activity. *Immunity* 52, 1075–1087.e8. <https://doi.org/10.1016/j.immuni.2020.05.001>.
9. Jeong, M., Cortopassi, F., See, J.X., De La Torre, C., Cerwenka, A., and Stojanovic, A. (2024). Vitamin A-treated natural killer cells reduce interferon-gamma production and support regulatory T-cell differentiation. *Eur. J. Immunol.* 54, e2250342. <https://doi.org/10.1002/eji.202250342>.
10. Krzywinska, E., and Stockmann, C. (2018). Hypoxia, Metabolism and Immune Cell Function. *Biomedicines* 6, 56. <https://doi.org/10.3390/biomedicines6020056>.
11. Carreau, A., El Hafny-Rahbi, B., Matejuk, A., Grillon, C., and Kieda, C. (2011). Why is the partial oxygen pressure of human tissues a crucial parameter? Small molecules and hypoxia. *J. Cell Mol. Med.* 15, 1239–1253. <https://doi.org/10.1111/j.1582-4934.2011.01258.x>.
12. Yuen, V.W.H., and Wong, C.C.L. (2020). Hypoxia-inducible factors and innate immunity in liver cancer. *J. Clin. Investig.* 130, 5052–5062. <https://doi.org/10.1172/jci137553>.
13. Chen, Z., Han, F., Du, Y., Shi, H., and Zhou, W. (2023). Hypoxic microenvironment in cancer: molecular mechanisms and therapeutic interventions. *Signal Transduct. Target. Ther.* 8, 70. <https://doi.org/10.1038/s41392-023-01332-8>.
14. Semenza, G.L. (2003). Targeting HIF-1 for cancer therapy. *Nat. Rev. Cancer* 3, 721–732. <https://doi.org/10.1038/nrc1187>.
15. Kennedy, P.R., Arvindam, U.S., Phung, S.K., Ettestad, B., Feng, X., Li, Y., Kile, Q.M., Hinderlie, P., Khaw, M., Huang, R.S., et al. (2024). Metabolic programs drive function of therapeutic NK cells in hypoxic tumor environments. *Sci. Adv.* 10, eadn1849. <https://doi.org/10.1126/sciadv.adn1849>.
16. Palazon, A., Tyrakis, P.A., Macias, D., Veliça, P., Rundqvist, H., Fitzpatrick, S., Vojnovic, N., Phan, A.T., Loman, N., Hedenfalk, I., et al. (2017). An HIF-1 α /VEGF-A Axis in Cytotoxic T Cells Regulates Tumor Progression. *Cancer Cell* 32, 669–683.e5. <https://doi.org/10.1016/j.ccell.2017.10.003>.
17. Shen, H., Ojo, O.A., Ding, H., Mullen, L.J., Xing, C., Hossain, M.I., Yassin, A., Shi, V.Y., Lewis, Z., Podgorska, E., et al. (2024). HIF1 α -regulated glycolysis promotes activation-induced cell death and IFN- γ induction

- in hypoxic T cells. *Nat. Commun.* 15, 9394. <https://doi.org/10.1038/s41467-024-53593-8>.
18. Krzywinska, E., Kantari-Mimoun, C., Kerdiles, Y., Sobocki, M., Isagawa, T., Gotthardt, D., Castells, M., Haubold, J., Millien, C., Viel, T., et al. (2017). Loss of HIF-1 α in natural killer cells inhibits tumour growth by stimulating non-productive angiogenesis. *Nat. Commun.* 8, 1597. <https://doi.org/10.1038/s41467-017-01599-w>.
 19. Victorino, F., Bigley, T.M., Park, E., Yao, C.H., Benoit, J., Yang, L.P., Piersma, S.J., Lauron, E.J., Davidson, R.M., Patti, G.J., and Yokoyama, W.M. (2021). HIF1 α is required for NK cell metabolic adaptation during virus infection. *eLife* 10, e68484. <https://doi.org/10.7554/eLife.68484>.
 20. Sobocki, M., Krzywinska, E., Nagarajan, S., Audigé, A., Huynh, K., Zachary, J., Debbache, J., Kerdiles, Y., Gotthardt, D., Takeda, N., et al. (2021). NK cells in hypoxic skin mediate a trade-off between wound healing and antibacterial defence. *Nat. Commun.* 12, 4700. <https://doi.org/10.1038/s41467-021-25065-w>.
 21. Semenza, G.L. (2017). A compendium of proteins that interact with HIF-1 α . *Exp. Cell Res.* 356, 128–135. <https://doi.org/10.1016/j.yexcr.2017.03.041>.
 22. Kallio, P.J., Pongratz, I., Gradin, K., McGuire, J., and Poellinger, L. (1997). Activation of hypoxia-inducible factor 1 α : posttranscriptional regulation and conformational change by recruitment of the Arnt transcription factor. *Proc. Natl. Acad. Sci. USA* 94, 5667–5672. <https://doi.org/10.1073/pnas.94.11.5667>.
 23. Arany, Z., Huang, L.E., Eckner, R., Bhattacharya, S., Jiang, C., Goldberg, M.A., Bunn, H.F., and Livingston, D.M. (1996). An essential role for p300/CBP in the cellular response to hypoxia. *Proc. Natl. Acad. Sci. USA* 93, 12969–12973. <https://doi.org/10.1073/pnas.93.23.12969>.
 24. Kobayashi, A., Numayama-Tsuruta, K., Sogawa, K., and Fujii-Kuriyama, Y. (1997). CBP/p300 functions as a possible transcriptional coactivator of Ah receptor nuclear translocator (Arnt). *J. Biochem.* 122, 703–710. <https://doi.org/10.1093/oxfordjournals.jbchem.a021812>.
 25. Hayashi, S., Watanabe, J., Nakachi, K., Eguchi, H., Gotoh, O., and Kawajiri, K. (1994). Interindividual difference in expression of human Ah receptor and related P450 genes. *Carcinogenesis* 15, 801–806. <https://doi.org/10.1093/carcin/15.5.801>.
 26. Stockinger, B., Di Meglio, P., Gialitakis, M., and Duarte, J.H. (2014). The aryl hydrocarbon receptor: multitasking in the immune system. *Annu. Rev. Immunol.* 32, 403–432. <https://doi.org/10.1146/annurev-immunol-032713-120245>.
 27. Mezrich, J.D., Fechner, J.H., Zhang, X., Johnson, B.P., Burlingham, W.J., and Bradfield, C.A. (2010). An interaction between kynurenine and the aryl hydrocarbon receptor can generate regulatory T cells. *J. Immunol.* 185, 3190–3198. <https://doi.org/10.4049/jimmunol.0903670>.
 28. Nguyen, N.T., Kimura, A., Nakahama, T., Chinen, I., Masuda, K., Nohara, K., Fujii-Kuriyama, Y., and Kishimoto, T. (2010). Aryl hydrocarbon receptor negatively regulates dendritic cell immunogenicity via a kynurenine-dependent mechanism. *Proc. Natl. Acad. Sci. USA* 107, 19961–19966. <https://doi.org/10.1073/pnas.1014465107>.
 29. Kiss, E.A., Vonarbourg, C., Kopfmann, S., Hobeika, E., Finke, D., Esser, C., and Diefenbach, A. (2011). Natural aryl hydrocarbon receptor ligands control organogenesis of intestinal lymphoid follicles. *Science* 334, 1561–1565. <https://doi.org/10.1126/science.1214914>.
 30. Moura-Alves, P., Faé, K., Houthuys, E., Dorhoi, A., Kreuchwig, A., Ferkert, J., Barison, N., Diehl, A., Munder, A., Constant, P., et al. (2014). AhR sensing of bacterial pigments regulates antibacterial defence. *Nature* 512, 387–392. <https://doi.org/10.1038/nature13684>.
 31. Shin, J.H., Zhang, L., Murillo-Sauca, O., Kim, J., Kohrt, H.E.K., Bui, J.D., and Sunwoo, J.B. (2013). Modulation of natural killer cell antitumor activity by the aryl hydrocarbon receptor. *Proc. Natl. Acad. Sci. USA* 110, 12391–12396. <https://doi.org/10.1073/pnas.1302856110>.
 32. Shin, J.H., Moreno-Nieves, U.Y., Zhang, L.H., Chen, C., Dixon, A.L., Linde, M.H., Mace, E.M., and Sunwoo, J.B. (2021). AHR Regulates NK Cell Migration via ASB2-Mediated Ubiquitination of Filamin A. *Front. Immunol.* 12, 624284. <https://doi.org/10.3389/fimmu.2021.624284>.
 33. Trikha, P., Moseman, J.E., Thakkar, A., Campbell, A.R., Elmas, E., Foltz, J.A., Chakravarti, N., Fitch, J.R., Mardis, E.R., and Lee, D.A. (2021). Defining the AHR-regulated transcriptome in NK cells reveals gene expression programs relevant to development and function. *Blood Adv.* 5, 4605–4618. <https://doi.org/10.1182/bloodadvances.2021004533>.
 34. Hughes, T., Briercheck, E.L., Freud, A.G., Trotta, R., McClory, S., Scoville, S.D., Keller, K., Deng, Y., Cole, J., Harrison, N., et al. (2014). The transcription factor AHR prevents the differentiation of a stage 3 innate lymphoid cell subset to natural killer cells. *Cell Rep.* 8, 150–162. <https://doi.org/10.1016/j.celrep.2014.05.042>.
 35. Moreno-Nieves, U.Y., Mundy, D.C., Shin, J.H., Tam, K., and Sunwoo, J.B. (2018). The aryl hydrocarbon receptor modulates the function of human CD56(bright) NK cells. *Eur. J. Immunol.* 48, 771–776. <https://doi.org/10.1002/eji.201747289>.
 36. Mascanfroni, I.D., Takenaka, M.C., Yeste, A., Patel, B., Wu, Y., Kenison, J.E., Siddiqui, S., Basso, A.S., Otterbein, L.E., Pardoll, D.M., et al. (2015). Metabolic control of type 1 regulatory T cell differentiation by AHR and HIF1- α . *Nat. Med.* 21, 638–646. <https://doi.org/10.1038/nm.3868>.
 37. Tomura, M., Zhou, X.Y., Maruo, S., Ahn, H.J., Hamaoka, T., Okamura, H., Nakanishi, K., Tanimoto, T., Kurimoto, M., and Fujiwara, H. (1998). A critical role for IL-18 in the proliferation and activation of NK1.1+ CD3- cells. *J. Immunol.* 160, 4738–4746.
 38. Takeda, K., Tsutsui, H., Yoshimoto, T., Adachi, O., Yoshida, N., Kishimoto, T., Okamura, H., Nakanishi, K., and Akira, S. (1998). Defective NK cell activity and Th1 response in IL-18-deficient mice. *Immunity* 8, 383–390. [https://doi.org/10.1016/s1074-7613\(00\)80543-9](https://doi.org/10.1016/s1074-7613(00)80543-9).
 39. Tsutsui, H., Nakanishi, K., Matsui, K., Higashino, K., Okamura, H., Miyazawa, Y., and Kaneda, K. (1996). IFN- γ -inducing factor up-regulates Fas ligand-mediated cytotoxic activity of murine natural killer cell clones. *J. Immunol.* 157, 3967–3973.
 40. Kobayashi, K., Hernandez, L.D., Galán, J.E., Janeway, C.A., Jr., Medzhitov, R., and Flavell, R.A. (2002). IRAK-M is a negative regulator of Toll-like receptor signaling. *Cell* 110, 191–202. [https://doi.org/10.1016/s0092-8674\(02\)00827-9](https://doi.org/10.1016/s0092-8674(02)00827-9).
 41. Arase, N., Arase, H., Park, S.Y., Ohno, H., Ra, C., and Saito, T. (1997). Association with Fc γ R3 is essential for activation signal through NKR-P1 (CD161) in natural killer (NK) cells and NK1.1+ T cells. *J. Exp. Med.* 186, 1957–1963. <https://doi.org/10.1084/jem.186.12.1957>.
 42. Aguilar, O.A., Fong, L.K., and Lanier, L.L. (2024). ITAM-based receptors in natural killer cells. *Immunol. Rev.* 323, 40–53. <https://doi.org/10.1111/immr.13313>.
 43. Badia-I-Mompel, P., Vélez Santiago, J., Braunger, J., Geiss, C., Dimitrov, D., Müller-Dott, S., Taus, P., Dugourd, A., Holland, C.H., Ramirez Flores, R.O., and Saez-Rodriguez, J. (2022). decoupler: ensemble of computational methods to infer biological activities from omics data. *Bioinform. Adv.* 2, vbac016. <https://doi.org/10.1093/bioadv/vbac016>.
 44. Heath-Pagliuso, S., Rogers, W.J., Tullis, K., Seidel, S.D., Cenijn, P.H., Brouwer, A., and Denison, M.S. (1998). Activation of the Ah receptor by tryptophan and tryptophan metabolites. *Biochemistry* 37, 11508–11515. <https://doi.org/10.1021/bi980087p>.
 45. Veldhoen, M., Hirota, K., Christensen, J., O'Garra, A., and Stockinger, B. (2009). Natural agonists for aryl hydrocarbon receptor in culture medium are essential for optimal differentiation of Th17 T cells. *J. Exp. Med.* 206, 43–49. <https://doi.org/10.1084/jem.20081438>.
 46. Diani-Moore, S., Ram, P., Li, X., Mondal, P., Youn, D.Y., Sauve, A.A., and Rifkind, A.B. (2010). Identification of the aryl hydrocarbon receptor target gene TIPARP as a mediator of suppression of hepatic gluconeogenesis by 2,3,7,8-tetrachlorodibenzo-p-dioxin and of nicotinamide as a corrective agent for this effect. *J. Biol. Chem.* 285, 38801–38810. <https://doi.org/10.1074/jbc.M110.131573>.

47. Xu, C., Li, C.Y.T., and Kong, A.N.T. (2005). Induction of phase I, II and III drug metabolism/transport by xenobiotics. *Arch Pharm. Res. (Seoul)* **28**, 249–268. <https://doi.org/10.1007/bf02977789>.
48. Nguyen, C.H., Brenner, S., Huttary, N., Atanasov, A.G., Dirsch, V.M., Chatuphonprasert, W., Holzner, S., Stadler, S., Riha, J., Krieger, S., et al. (2016). AHR/CYP1A1 interplay triggers lymphatic barrier breaching in breast cancer spheroids by inducing 12(S)-HETE synthesis. *Hum. Mol. Genet.* **25**, 5006–5016. <https://doi.org/10.1093/hmg/ddw329>.
49. Vogel, C.F.A., Sciuillo, E., Li, W., Wong, P., Lazennec, G., and Matsuura, F. (2007). RelB, a new partner of aryl hydrocarbon receptor-mediated transcription. *Mol. Endocrinol.* **21**, 2941–2955. <https://doi.org/10.1210/me.2007-0211>.
50. Miyake, T., Satoh, T., Kato, H., Matsushita, K., Kumagai, Y., Vandenbon, A., Tani, T., Muta, T., Akira, S., and Takeuchi, O. (2010). $\text{I}\kappa\text{B}\zeta$ is essential for natural killer cell activation in response to IL-12 and IL-18. *Proc. Natl. Acad. Sci. USA* **107**, 17680–17685. <https://doi.org/10.1073/pnas.1012977107>.
51. Loftus, R.M., Assmann, N., Kedia-Mehta, N., O'Brien, K.L., Garcia, A., Gillespie, C., Hukelmann, J.L., Oefner, P.J., Lamond, A.I., Gardiner, C.M., et al. (2018). Amino acid-dependent cMyc expression is essential for NK cell metabolic and functional responses in mice. *Nat. Commun.* **9**, 2341. <https://doi.org/10.1038/s41467-018-04719-2>.
52. Kannan, Y., Yu, J., Raices, R.M., Seshadri, S., Wei, M., Caligiuri, M.A., and Wewers, M.D. (2011). $\text{I}\kappa\text{B}\zeta$ augments IL-12- and IL-18-mediated IFN- γ production in human NK cells. *Blood* **117**, 2855–2863. <https://doi.org/10.1182/blood-2010-07-294702>.
53. Tang, F., Li, J., Qi, L., Liu, D., Bo, Y., Qin, S., Miao, Y., Yu, K., Hou, W., Li, J., et al. (2023). A pan-cancer single-cell panorama of human natural killer cells. *Cell* **186**, 4235–4251.e20. <https://doi.org/10.1016/j.cell.2023.07.034>.
54. Schmidt, J.R., Haupt, J., Riemschneider, S., Kämpf, C., Löffler, D., Blumert, C., Reiche, K., Koehl, U., Kalkhof, S., and Lehmann, J. (2023). Transcriptomic signatures reveal a shift towards an anti-inflammatory gene expression profile but also the induction of type I and type II interferon signaling networks through aryl hydrocarbon receptor activation in murine macrophages. *Front. Immunol.* **14**, 1156493. <https://doi.org/10.3389/fimmu.2023.1156493>.
55. Kadow, S., Jux, B., Zahner, S.P., Wingerath, B., Chmill, S., Clausen, B.E., Hengstler, J., and Esser, C. (2011). Aryl hydrocarbon receptor is critical for homeostasis of invariant $\gamma\delta$ T cells in the murine epidermis. *J. Immunol.* **187**, 3104–3110. <https://doi.org/10.4049/jimmunol.1100912>.
56. Semenza, G.L., Jiang, B.H., Leung, S.W., Passantino, R., Concordet, J.P., Maire, P., and Giallongo, A. (1996). Hypoxia response elements in the aldolase A, enolase 1, and lactate dehydrogenase A gene promoters contain essential binding sites for hypoxia-inducible factor 1. *J. Biol. Chem.* **271**, 32529–32537. <https://doi.org/10.1074/jbc.271.51.32529>.
57. Cho, S.S., Bacon, C.M., Sudarshan, C., Rees, R.C., Finbloom, D., Pine, R., and O'Shea, J.J. (1996). Activation of STAT4 by IL-12 and IFN- α : evidence for the involvement of ligand-induced tyrosine and serine phosphorylation. *J. Immunol.* **157**, 4781–4789.
58. Klein, J.L., Fickenscher, H., Holliday, J.E., Biesinger, B., and Fleckenstein, B. (1996). Herpesvirus saimiri immortalized gamma delta T cell line activated by IL-12. *J. Immunol.* **156**, 2754–2760.
59. Dérjard, B., Raingeaud, J., Barrett, T., Wu, I.H., Han, J., Ulevitch, R.J., and Davis, R.J. (1995). Independent human MAP-kinase signal transduction pathways defined by MEK and MKK isoforms. *Science* **267**, 682–685. <https://doi.org/10.1126/science.7839144>.
60. Visconti, R., Gadina, M., Chiariello, M., Chen, E.H., Stancato, L.F., Gutkind, J.S., and O'Shea, J.J. (2000). Importance of the MKK6/p38 pathway for interleukin-12-induced STAT4 serine phosphorylation and transcriptional activity. *Blood* **96**, 1844–1852.
61. Goh, K.C., Haque, S.J., and Williams, B.R. (1999). p38 MAP kinase is required for STAT1 serine phosphorylation and transcriptional activation induced by interferons. *Embo j* **18**, 5601–5608. <https://doi.org/10.1093/emboj/18.20.5601>.
62. Mavropoulos, A., Sully, G., Cope, A.P., and Clark, A.R. (2005). Stabilization of IFN- γ mRNA by MAPK p38 in IL-12- and IL-18-stimulated human NK cells. *Blood* **105**, 282–288. <https://doi.org/10.1182/blood-2004-07-2782>.
63. Saha, R.N., Jana, M., and Pahan, K. (2007). MAPK p38 regulates transcriptional activity of NF- κ B in primary human astrocytes via acetylation of p65. *J. Immunol.* **179**, 7101–7109. <https://doi.org/10.4049/jimmunol.179.10.7101>.
64. Labuda, T., Sundstedt, A., and Dohlstien, M. (2000). Selective induction of p38 mitogen-activated protein kinase activity following A6H co-stimulation in primary human CD4(+) T cells. *Int. Immunol.* **12**, 253–261. <https://doi.org/10.1093/intimm/12.3.253>.
65. Puccetti, P., Fallarino, F., Italiano, A., Soubeyran, I., MacGrogan, G., Debled, M., Velasco, V., Bodet, D., Eimer, S., Veldhoen, M., et al. (2015). Accumulation of an endogenous tryptophan-derived metabolite in colorectal and breast cancers. *PLoS One* **10**, e0122046. <https://doi.org/10.1371/journal.pone.0122046>.
66. Opitz, C.A., Litzenburger, U.M., Sahn, F., Ott, M., Tritschler, I., Trump, S., Schumacher, T., Jestaedt, L., Schrenk, D., Weller, M., et al. (2011). An endogenous tumour-promoting ligand of the human aryl hydrocarbon receptor. *Nature* **478**, 197–203. <https://doi.org/10.1038/nature10491>.
67. Laskowski, T.J., Biederstädt, A., and Rezvani, K. (2022). Natural killer cells in antitumour adoptive cell immunotherapy. *Nat. Rev. Cancer* **22**, 557–575. <https://doi.org/10.1038/s41568-022-00491-0>.
68. Morvan, M.G., and Lanier, L.L. (2016). NK cells and cancer: you can teach innate cells new tricks. *Nat. Rev. Cancer* **16**, 7–19. <https://doi.org/10.1038/nrc.2015.5>.
69. Prager, I., and Watzl, C. (2019). Mechanisms of natural killer cell-mediated cellular cytotoxicity. *J. Leukoc. Biol.* **105**, 1319–1329. <https://doi.org/10.1002/jlb.Mr0718-269r>.
70. Fauriat, C., Long, E.O., Ljunggren, H.G., and Bryceson, Y.T. (2010). Regulation of human NK-cell cytokine and chemokine production by target cell recognition. *Blood* **115**, 2167–2176. <https://doi.org/10.1182/blood-2009-08-238469>.
71. Piersma, S.J., Pak-Wittel, M.A., Lin, A., Plougastel-Douglas, B., and Yokoyama, W.M. (2019). Activation Receptor-Dependent IFN- γ Production by NK Cells Is Controlled by Transcription, Translation, and the Proteasome. *J. Immunol.* **203**, 1981–1988. <https://doi.org/10.4049/jimmunol.1900718>.
72. Littwitz-Salomon, E., Moreira, D., Frost, J.N., Choi, C., Liou, K.T., Ahern, D.K., O'Shaughnessy, S., Wagner, B., Biron, C.A., Drakesmith, H., et al. (2021). Metabolic requirements of NK cells during the acute response against retroviral infection. *Nat. Commun.* **12**, 5376. <https://doi.org/10.1038/s41467-021-25715-z>.
73. Terrén, I., Orrantia, A., Vitallé, J., Zenarruzabeitia, O., and Borrego, F. (2019). NK Cell Metabolism and Tumor Microenvironment. *Front. Immunol.* **10**, 2278. <https://doi.org/10.3389/fimmu.2019.02278>.
74. Li, L., Mohanty, V., Dou, J., Huang, Y., Banerjee, P.P., Miao, Q., Lohr, J.G., Vijaykumar, T., Frede, J., Knoechel, B., et al. (2023). Loss of metabolic fitness drives tumor resistance after CAR-NK cell therapy and can be overcome by cytokine engineering. *Sci. Adv.* **9**, eadd6997. <https://doi.org/10.1126/sciadv.add6997>.
75. Balsamo, M., Manzini, C., Pietra, G., Raggi, F., Blengio, F., Mingari, M.C., Varesio, L., Moretta, L., Bosco, M.C., and Vitale, M. (2013). Hypoxia downregulates the expression of activating receptors involved in NK-cell-mediated target cell killing without affecting ADCC. *Eur. J. Immunol.* **43**, 2756–2764. <https://doi.org/10.1002/eji.201343448>.
76. Parodi, M., Raggi, F., Cangelosi, D., Manzini, C., Balsamo, M., Blengio, F., Eva, A., Varesio, L., Pietra, G., Moretta, L., et al. (2018). Hypoxia Modifies the Transcriptome of Human NK Cells, Modulates Their Immunoregulatory Profile, and Influences NK Cell Subset Migration. *Front. Immunol.* **9**, 2358. <https://doi.org/10.3389/fimmu.2018.02358>.

77. Cramer, L.A., Nelson, S.L., and Klemsz, M.J. (2000). Synergistic induction of the Tap-1 gene by IFN-gamma and lipopolysaccharide in macrophages is regulated by STAT1. *J. Immunol.* *165*, 3190–3197. <https://doi.org/10.4049/jimmunol.165.6.3190>.
78. Nathan, C.F., Murray, H.W., Wiebe, M.E., and Rubín, B.Y. (1983). Identification of interferon-gamma as the lymphokine that activates human macrophage oxidative metabolism and antimicrobial activity. *J. Exp. Med.* *158*, 670–689. <https://doi.org/10.1084/jem.158.3.670>.
79. Curtsinger, J.M., Agarwal, P., Lins, D.C., and Mescher, M.F. (2012). Autocrine IFN- γ promotes naive CD8 T cell differentiation and synergizes with IFN- α to stimulate strong function. *J. Immunol.* *189*, 659–668. <https://doi.org/10.4049/jimmunol.1102727>.
80. Martín-Fontecha, A., Thomsen, L.L., Brett, S., Gerard, C., Lipp, M., Lanzavecchia, A., and Sallusto, F. (2004). Induced recruitment of NK cells to lymph nodes provides IFN-gamma for T(H)1 priming. *Nat. Immunol.* *5*, 1260–1265. <https://doi.org/10.1038/ni1138>.
81. Cimpean, M., Keppel, M.P., Gainullina, A., Fan, C., Sohn, H., Schedler, N.C., Swain, A., Kolicheki, A., Shapiro, H., Young, H.A., et al. (2023). IL-15 Priming Alters IFN- γ Regulation in Murine NK Cells. *J. Immunol.* *211*, 1481–1493. <https://doi.org/10.4049/jimmunol.2300283>.
82. Hodge, D.L., Martínez, A., Julias, J.G., Taylor, L.S., and Young, H.A. (2002). Regulation of nuclear gamma interferon gene expression by interleukin 12 (IL-12) and IL-2 represents a novel form of posttranscriptional control. *Mol. Cell Biol.* *22*, 1742–1753. <https://doi.org/10.1128/mcb.22.6.1742-1753.2002>.
83. Luetke-Eversloh, M., Hammer, Q., Durek, P., Nordström, K., Gasparoni, G., Pink, M., Hamann, A., Walter, J., Chang, H.D., Dong, J., and Romagnani, C. (2014). Human cytomegalovirus drives epigenetic imprinting of the IFNG locus in NKG2Chi natural killer cells. *PLoS Pathog.* *10*, e1004441. <https://doi.org/10.1371/journal.ppat.1004441>.
84. Kunikata, T., Torigoe, K., Ushio, S., Okura, T., Ushio, C., Yamauchi, H., Ikeda, M., Ikegami, H., and Kurimoto, M. (1998). Constitutive and induced IL-18 receptor expression by various peripheral blood cell subsets as determined by anti-hIL-18R monoclonal antibody. *Cell. Immunol.* *189*, 135–143. <https://doi.org/10.1006/cimm.1998.1376>.
85. Yoshimoto, T., Takeda, K., Tanaka, T., Ohkusu, K., Kashiwamura, S., Okamura, H., Akira, S., and Nakanishi, K. (1998). IL-12 up-regulates IL-18 receptor expression on T cells, Th1 cells, and B cells: synergism with IL-18 for IFN-gamma production. *J. Immunol.* *161*, 3400–3407.
86. Nandagopal, N., Ali, A.K., Komal, A.K., and Lee, S.H. (2014). The Critical Role of IL-15-PI3K-mTOR Pathway in Natural Killer Cell Effector Functions. *Front. Immunol.* *5*, 187. <https://doi.org/10.3389/fimmu.2014.00187>.
87. Khameneh, H.J., Fonta, N., Zenobi, A., Niogret, C., Ventura, P., Guerra, C., Kwee, I., Rinaldi, A., Pecoraro, M., Geiger, R., et al. (2023). Myc controls NK cell development, IL-15-driven expansion, and translational machinery. *Life Sci. Alliance* *6*, e202302069. <https://doi.org/10.26508/lsa.202302069>.
88. Marçais, A., Cherfils-Vicini, J., Viant, C., Degouve, S., Viel, S., Fenis, A., Rabilloud, J., Mayol, K., Tavares, A., Bienvenu, J., et al. (2014). The metabolic checkpoint kinase mTOR is essential for IL-15 signaling during the development and activation of NK cells. *Nat. Immunol.* *15*, 749–757. <https://doi.org/10.1038/ni.2936>.
89. Marçais, A., Viel, S., Grau, M., Henry, T., Marvel, J., and Walzer, T. (2013). Regulation of mouse NK cell development and function by cytokines. *Front. Immunol.* *4*, 450. <https://doi.org/10.3389/fimmu.2013.00450>.
90. Donnelly, R.P., Loftus, R.M., Keating, S.E., Liou, K.T., Biron, C.A., Gardiner, C.M., and Finlay, D.K. (2014). mTORC1-dependent metabolic reprogramming is a prerequisite for NK cell effector function. *J. Immunol.* *193*, 4477–4484. <https://doi.org/10.4049/jimmunol.1401558>.
91. Assmann, N., O'Brien, K.L., Donnelly, R.P., Dyck, L., Zaiatz-Bittencourt, V., Loftus, R.M., Heinrich, P., Oefner, P.J., Lynch, L., Gardiner, C.M., et al. (2017). Srebp-controlled glucose metabolism is essential for NK cell functional responses. *Nat. Immunol.* *18*, 1197–1206. <https://doi.org/10.1038/ni.3838>.
92. Panwar, V., Singh, A., Bhatt, M., Tonk, R.K., Azizov, S., Raza, A.S., Sengupta, S., Kumar, D., and Garg, M. (2023). Multifaceted role of mTOR (mammalian target of rapamycin) signaling pathway in human health and disease. *Signal Transduct. Target. Ther.* *8*, 375. <https://doi.org/10.1038/s41392-023-01608-z>.
93. Sinclair, L.V., Neyens, D., Ramsay, G., Taylor, P.M., and Cantrell, D.A. (2018). Single cell analysis of kynurenine and System L amino acid transport in T cells. *Nat. Commun.* *9*, 1981. <https://doi.org/10.1038/s41467-018-04366-7>.
94. Rejano-Gordillo, C., Ordiales-Talavera, A., Nacarino-Palma, A., Merino, J.M., González-Rico, F.J., and Fernández-Salguero, P.M. (2022). Aryl Hydrocarbon Receptor: From Homeostasis to Tumor Progression. *Front. Cell Dev. Biol.* *10*, 884004. <https://doi.org/10.3389/fcell.2022.884004>.
95. Holfelder, P., Hensen, L., Prentzell, M.T., Navas, P.R., Solvay, M., Sadik, A., Sayeram, D., Rehbein, U., Bausbacher, T., Egger, A.-S., et al. (2024). The MTORC1-AHR pathway sustains translation and autophagy in tumours under tryptophan stress. Preprint at bioRxiv. <https://doi.org/10.1101/2023.01.16.523931>.
96. Alpsoy, A., Wu, X.S., Pal, S., Klingbeil, O., Kumar, P., El Demerdash, O., Nalbant, B., and Vakoc, C.R. (2024). I κ B ζ is a dual-use coactivator of NF- κ B and POU transcription factors. *Mol. Cell* *84*, 1149–1157.e7. <https://doi.org/10.1016/j.molcel.2024.01.007>.
97. Johansen, C., Mose, M., Ommen, P., Bertelsen, T., Vinter, H., Hailfinger, S., Lorscheid, S., Schulze-Osthoff, K., and Iversen, L. (2015). I κ B ζ is a key driver in the development of psoriasis. *Proc. Natl. Acad. Sci. USA* *112*, E5825–E5833. <https://doi.org/10.1073/pnas.1509971112>.
98. Feng, Y., Chen, Z., Xu, Y., Han, Y., Jia, X., Wang, Z., Zhang, N., and Lv, W. (2023). The central inflammatory regulator I κ B ζ : induction, regulation and physiological functions. *Front. Immunol.* *14*, 1188253. <https://doi.org/10.3389/fimmu.2023.1188253>.
99. Wang, W., Wykrzykowska, J., Johnson, T., Sen, R., and Sen, J. (1999). A NF-kappa B/c-myc-dependent survival pathway is targeted by corticosteroids in immature thymocytes. *J. Immunol.* *162*, 314–322.
100. Xu, W., Berning, P., Erdmann, T., Grau, M., Bettazová, N., Zapukhlyak, M., Frontzek, F., Kosnopfel, C., Lenz, P., Grondine, M., et al. (2023). mTOR inhibition amplifies the anti-lymphoma effect of PI3K β / δ blockage in diffuse large B-cell lymphoma. *Leukemia* *37*, 178–189. <https://doi.org/10.1038/s41375-022-01749-0>.
101. Singhal, R., and Shah, Y.M. (2020). Oxygen battle in the gut: Hypoxia and hypoxia-inducible factors in metabolic and inflammatory responses in the intestine. *J. Biol. Chem.* *295*, 10493–10505. <https://doi.org/10.1074/jbc.REV120.011188>.
102. Stockinger, B., Shah, K., and Wincent, E. (2021). AHR in the intestinal microenvironment: safeguarding barrier function. *Nat. Rev. Gastroenterol. Hepatol.* *18*, 559–570. <https://doi.org/10.1038/s41575-021-00430-8>.
103. Vondráček, J., and Machala, M. (2016). Environmental Ligands of the Aryl Hydrocarbon Receptor and Their Effects in Models of Adult Liver Progenitor Cells. *Stem Cells Int.* *2016*, 4326194. <https://doi.org/10.1155/2016/4326194>.
104. Martini, T., Naef, F., and Tchorz, J.S. (2023). Spatiotemporal Metabolic Liver Zonation and Consequences on Pathophysiology. *Annu. Rev. Pathol.* *18*, 439–466. <https://doi.org/10.1146/annurev-pathmechdis-031521-024831>.
105. van der Goot, A.T., and Nollen, E.A.A. (2013). Tryptophan metabolism: entering the field of aging and age-related pathologies. *Trends Mol. Med.* *19*, 336–344. <https://doi.org/10.1016/j.molmed.2013.02.007>.
106. Agus, A., Planchais, J., and Sokol, H. (2018). Gut Microbiota Regulation of Tryptophan Metabolism in Health and Disease. *Cell Host Microbe* *23*, 716–724. <https://doi.org/10.1016/j.chom.2018.05.003>.

107. Kelly, B., and Pearce, E.L. (2020). Amino Assets: How Amino Acids Support Immunity. *Cell Metab.* *32*, 154–175. <https://doi.org/10.1016/j.cmet.2020.06.010>.
108. Madera, S., and Sun, J.C. (2015). Cutting edge: stage-specific requirement of IL-18 for antiviral NK cell expansion. *J. Immunol.* *194*, 1408–1412. <https://doi.org/10.4049/jimmunol.1402001>.
109. Andrews, D.M., Scaizo, A.A., Yokoyama, W.M., Smyth, M.J., and Degli-Esposti, M.A. (2003). Functional interactions between dendritic cells and NK cells during viral infection. *Nat. Immunol.* *4*, 175–181. <https://doi.org/10.1038/ni880>.
110. Opitz, C.A., Somarribas Patterson, L.F., Mohapatra, S.R., Dewi, D.L., Sadiq, A., Platten, M., and Trump, S. (2020). The therapeutic potential of targeting tryptophan catabolism in cancer. *Br. J. Cancer* *122*, 30–44. <https://doi.org/10.1038/s41416-019-0664-6>.
111. Campesato, L.F., Budhu, S., Tchaicha, J., Weng, C.H., Gigoux, M., Cohen, I.J., Redmond, D., Mangarin, L., Pourpe, S., Liu, C., et al. (2020). Blockade of the AHR restricts a Treg-macrophage suppressive axis induced by L-Kynurenine. *Nat. Commun.* *11*, 4011. <https://doi.org/10.1038/s41467-020-17750-z>.
112. Solvay, M., Holfelder, P., Klaessens, S., Pilotte, L., Stroobant, V., Lamy, J., Naulaerts, S., Spillier, Q., Frédérick, R., De Plaen, E., et al. (2023). Tryptophan depletion sensitizes the AHR pathway by increasing AHR expression and GCN2/LAT1-mediated kynurenine uptake, and potentiates induction of regulatory T lymphocytes. *J. Immunother. Cancer* *11*, e006728. <https://doi.org/10.1136/jitc-2023-006728>.
113. Shinde, R., and McGaha, T.L. (2018). The Aryl Hydrocarbon Receptor: Connecting Immunity to the Microenvironment. *Trends Immunol.* *39*, 1005–1020. <https://doi.org/10.1016/j.it.2018.10.010>.
114. Quintana, F.J., Murugaiyan, G., Farez, M.F., Mitsdoerffer, M., Tukpah, A.M., Burns, E.J., and Weiner, H.L. (2010). An endogenous aryl hydrocarbon receptor ligand acts on dendritic cells and T cells to suppress experimental autoimmune encephalomyelitis. *Proc. Natl. Acad. Sci. USA* *107*, 20768–20773. <https://doi.org/10.1073/pnas.1009201107>.
115. Kober, C., Roewe, J., Schmees, N., Roese, L., Roehn, U., Bader, B., Stoeckigt, D., Prinz, F., Gorjánácz, M., Roeder, H.G., et al. (2023). Targeting the aryl hydrocarbon receptor (AhR) with BAY 2416964: a selective small molecule inhibitor for cancer immunotherapy. *J. Immunother. Cancer* *11*, e007495. <https://doi.org/10.1136/jitc-2023-007495>.
116. Bray, N.L., Pimentel, H., Melsted, P., and Pachter, L. (2016). Near-optimal probabilistic RNA-seq quantification. *Nat. Biotechnol.* *34*, 525–527. <https://doi.org/10.1038/nbt.3519>.
117. Ritchie, M.E., Phipson, B., Wu, D., Hu, Y., Law, C.W., Shi, W., and Smyth, G.K. (2015). limma powers differential expression analyses for RNA-seq and microarray studies. *Nucleic Acids Res.* *43*, e47. <https://doi.org/10.1093/nar/gkv007>.
118. Hao, Y., Hao, S., Andersen-Nissen, E., Mauck, W.M., 3rd, Zheng, S., Butler, A., Lee, M.J., Wilk, A.J., Darby, C., Zager, M., et al. (2021). Integrated analysis of multimodal single-cell data. *Cell* *184*, 3573–3587.e29. <https://doi.org/10.1016/j.cell.2021.04.048>.
119. Kanehisa, M., and Goto, S. (2000). KEGG: kyoto encyclopedia of genes and genomes. *Nucleic Acids Res.* *28*, 27–30. <https://doi.org/10.1093/nar/28.1.27>.
120. Croft, D., O’Kelly, G., Wu, G., Haw, R., Gillespie, M., Matthews, L., Caudy, M., Garapati, P., Gopinath, G., Jassal, B., et al. (2011). Reactome: a database of reactions, pathways and biological processes. *Nucleic Acids Res.* *39*, D691–D697. <https://doi.org/10.1093/nar/gkq1018>.
121. Harris, M.A., Clark, J., Ireland, A., Lomax, J., Ashburner, M., Foulger, R., Eilbeck, K., Lewis, S., Marshall, B., Mungall, C., et al. (2004). The Gene Ontology (GO) database and informatics resource. *Nucleic Acids Res.* *32*, D258–D261. <https://doi.org/10.1093/nar/gkh036>.
122. Korsunsky, I., Millard, N., Fan, J., Slowikowski, K., Zhang, F., Wei, K., Baglaenko, Y., Brenner, M., Loh, P.R., and Raychaudhuri, S. (2019). Fast, sensitive and accurate integration of single-cell data with Harmony. *Nat. Methods* *16*, 1289–1296. <https://doi.org/10.1038/s41592-019-0619-0>.

STAR★METHODS

KEY RESOURCES TABLE

REAGENT or RESOURCE	SOURCE	IDENTIFIER
Antibodies		
anti-mouse IFN- γ Brilliant Violet™ 650™ (XMG1.2)	BioLegend	505832; RRID: AB_11142685
anti-mouse IFN- γ PE (XMG1.2)	BioLegend	505808; RRID: AB_315402
anti-mouse IFN- γ FITC (XMG1.2)	BioLegend	505806; RRID: AB_315399
anti-mouse IFN- γ PE-Cyanine7 (XMG1.2)	BioLegend	505826; RRID: AB_2295770
anti-mouse IFN- γ APC (XMG1.2)	BioLegend	505810; RRID: AB_315403
anti-mouse IL-18R α APC (A17071D)	BioLegend	157908; RRID: AB_2876539
anti-mouse Eomes Alexa Fluor™ 488 (Dan11mag)	Thermo Fisher Scientific	53-4875-82; RRID: AB_10854265
anti-mouse Eomes PE-Cyanine7 (Dan11mag)	Thermo Fisher Scientific	25-4875-82; RRID: AB_2573454
anti-mouse CD3 ϵ Brilliant Violet™ 421™ (145-2C11)	BioLegend	100335; RRID: AB_10898314
anti-mouse CD3 ϵ APC-Cyanine7 (145-2C11)	BioLegend	100330; RRID: AB_1877170
anti-mouse CD3 ϵ Brilliant Violet™ 785™ (145-2C11)	BioLegend	100355; RRID: AB_2565969
anti-mouse CD3 ϵ APC (145-2C11)	BioLegend	100312; AB_312676
anti-mouse I κ B ζ PerCP-eFluor™ 710 (LK2NAP)	Thermo Fisher Scientific	46-6801-82; RRID: AB_11149496
anti-mouse c-Myc/N-Myc PE (D84C12)	Cell Signaling Technology	35876S; RRID: AB_2631168
anti-mouse c-Myc Alexa Fluor™ 647 (E5Q6W)	Cell Signaling Technology	45606S
anti-mouse Phospho-S6 Ribosomal Protein (Ser ^{235/236}) Alexa Fluor™ 647 (D57.2.2E)	Cell Signaling Technology	4851
anti-mouse Phospho-S6 Ribosomal Protein (Ser ^{235/236}) PE (D57.2.2E)	Cell Signaling Technology	5316
anti-mouse NK1.1 Brilliant Violet™ 785™ (PK136)	BioLegend	108749; RRID: AB_2564304
anti-mouse NK1.1 PE (PK136)	BioLegend	108708; RRID: AB_313394
anti-mouse NK1.1 FITC (PK136)	BioLegend	108706; RRID: AB_313392
anti-mouse NK1.1 Brilliant Violet™ 421™ (PK136)	BioLegend	108732; RRID: AB_10895916
anti-mouse NK1.1 APC (PK136)	BioLegend	108710; RRID: AB_313396
anti-mouse NK1.1 PE-Cyanine7 (PK136)	BioLegend	108714; RRID: AB_389363

(Continued on next page)

Continued

REAGENT or RESOURCE	SOURCE	IDENTIFIER
Rat IgG1 Isotype control Brilliant Violet™ 650 (κRTK2071)	BioLegend	400438; RRID: AB_3097673
Rat IgG1 Isotype control PE (κRTK2071)	BioLegend	400408; RRID: AB_326514
Rat IgG1 Isotype control FITC (κRTK2071)	BioLegend	400406; RRID: AB_326512
Rat IgG1 Isotype control PE-Cy7 (κRTK2071)	BioLegend	400416; RRID: AB_326522
Rat IgG1 Isotype control APC (κRTK2071)	BioLegend	400412; RRID: AB_326518
IgG XP® Isotype Control PE (DA1E)	Cell Signaling Technology	5742
IgG XP® Isotype Control Alexa Fluor™ 647 (DA1E)	Cell Signaling Technology	2985S
IgG XP® Isotype Control Alexa Fluor™ 488 (DA1E)	Cell Signaling Technology	2975
Mouse IgG2a kappa Isotype Control PerCP-eFluor™ 710 (BM2a)	Thermo Fisher Scientific	46-4724-82; RRID: AB_1834451
Chemicals, peptides, and recombinant proteins		
10058-F4	Selleckhem	Cat#S7153
2-Mercaptoethanol	VWR	Cat#0482
2-Mercaptoethanol	Gibco	Cat#31350
Golgi Stop™	BDBiosciences	Cat#554724
Recombinant human IL-2	NIH	Cat#1104-0890
Recombinant mouse IL-12	Peptotech	Cat#210-12
Recombinant mouse IL-18	MBL International	Cat#B002-5
Torin2	Selleckhem	Cat#S2817
Zombie Aqua™ Fixable Viability Dye	Biolegend	Cat#423102
Cytofix/Cytoperm™ buffer	BD Biosciences	Cat#554714
Phosflow Perm buffer III™	BD Biosciences	Cat#558050
L-Kynurenine	Selleckhem	Cat#S5839
LEAF™ Purified anti-mouse NK1.1	Biolegend	Cat#108712
Critical commercial assays		
eBioscience™ FoxP3 Transcription Factor Staining Buffer Set	Invitrogen	Cat#00-5523-00
BD Cytofix/Cytoperm™ Fixation/Permeabilization Kit	BD Biosciences	Cat#554714
RNeasy® Mini Kit	QIAGEN	Cat#74104
Seahorse XF HS Mini FluxPak (PDL plates)	Aglient	Cat#103724-100
MACS® LS Columns	Miltenyi	Cat#130-042-401
Vybrant™ FLICA Caspase Apoptosis Assay Kit	Thermo Fischer Scientific	Cat#V35118
CellTrace™ Violet Cell Proliferation Kit	Thermo Fisher Scientific	Cat# C34557
Turbo DNA-free™ Kit	Thermo Fisher Scientific	Cat#AM1907
Deposited data		
NK cells cultured in normoxia or hypoxia	<i>This paper</i>	GEO: GSE292263
Control or gene-deficient NK cells cultured in hypoxia	<i>This paper</i>	GEO: GSE292264
Tumor-infiltrating control of Hif1a-deficient NK cells	Ni et al. ⁹ 2020	GEO: GSE123534
Experimental models: cell lines		
RMA-S	<i>In house</i>	NA

(Continued on next page)

Continued		
REAGENT or RESOURCE	SOURCE	IDENTIFIER
RMA-Rae1 γ	<i>In house</i>	NA
Experimental models: Organisms		
Mouse: C57BL/6N (C57BL/6NRj)	Janvier Labs	RRID:IMSR MGI:6236253
Mouse: B6(MF;129)-Rag2 ^{tm1Fwa}	<i>In house</i>	NA
Mouse: B6(MF;129)-Rag2 ^{tm1Fwa} Ptpca	<i>In house</i>	NA
Mouse: C57BL/B6-Tg(Ncr1-iCre) ^{265Sxl} Ahr ^{tm3.1Bra} Rag2 ^{tm1Fwa}	<i>In house</i>	NA
Mouse: C57BL/B6-Tg(Ncr1-iCre) ^{265Sxl} Ahr ^{tm3.1Bra}	<i>In house</i>	NA
Mouse: C57BL/6-Tg(Ncr1-iCre) ^{265Sxl} Hif1a ^{tm3Rsjo}	<i>In house</i>	NA
Mouse: C57BL/6-Tg(Ncr1-iCre) ^{265Sxl} Ahr ^{tm3.1Bra} Hif1a ^{tm3Rsjo}	<i>In house</i>	NA
Software and algorithms		
GraphPad Prism 7	GraphPad	https://www.graphpad.com/
FlowJo™ version >10.7.1	FlowJo™ LLC	https://www.flowjo.com/
R version \geq 4.3.1	R core team	https://www.r-project.org/
R studio version \geq 2023.09.01 build 494	Posit	https://posit.co/
Bioconductor version \geq 3.18	NA	https://bioconductor.org/
FastQC	Babraham Bioinformatics	https://www.bioinformatics.babraham.ac.uk/projects/fastqc/
trim_galore version 0.6.4	Babraham Bioinformatics	https://github.com/FelixKrueger/TrimGalore
Kallisto version 0.46.1	Bray et al. ¹¹⁶ 2016	https://pachterlab.github.io/kallisto/
Limma package	Ritchie et al. ¹¹⁷ 2015	https://bioconductor.org/packages/release/bioc/html/limma.html
Fgsea version 1.32.2	NA	https://bioconductor.org/packages/release/bioc/html/fgsea.html
Geneset version 0.2.7	NA	https://cran.r-project.org/web/packages/geneset/index.html
ggplot2 version 3.5.1	NA	https://ggplot2.tidyverse.org/
Enhanced Volcano version 1.20.0	NA	https://github.com/kevinblighe/EnhancedVolcano
Pheatmap version 1.0.12	NA	https://cran.rstudio.com/web/packages/pheatmap/index.html
VennDetail shiny app	NA	https://www.bioconductor.org/packages/devel/bioc/vignettes/VennDetail/inst/doc/VennDetail.html
DecoupleR version 2.9.7	Badia-I-Mompel et al. ⁴³ 2022	https://saezlab.github.io/decoupleR/
Seurat v4	Hao et al. ¹¹⁸ 2021	https://satijalab.org/seurat/index.html
Pan-NK cancer atlas	Tang et al. ⁵³ 2023	http://pan-nk.cancer-pku.cn

EXPERIMENTAL MODEL AND STUDY PARTICIPANT DETAILS

Mice

C57BL/6N wild-type (WT) mice were purchased from Janvier. Rag2-deficient mice, Ncr1^{iCre} Ahr^{fl/fl} (wild-type and Rag2-deficient), Ncr1^{iCre} Hif1a^{fl/fl} and Ncr1^{iCre} Ahr^{fl/fl} Hif1a^{fl/fl} mice were bred *in house*. Mice were housed at the Medical Faculty Mannheim under specific-pathogen-free conditions, and in accordance with all standards of animal care. Male and female mice were used for cell

isolation. Unless otherwise indicated, organs were pooled for cell isolation and downstream applications. All experiments were conducted using age- and sex-matched experimental groups (treatment and genotype), with mice between 10 and 40 weeks of age. Animal procedures and organ harvesting were authorized under internal licenses of the Medical Faculty Mannheim (I-23/31 and I-19/21).

Cell lines

RMA-S and RMA-Rae1 γ cells were maintained in RPMI-1664 medium supplemented with 10% FBS, 1% L-glutamine, and 1% Penicillin/Streptomycin (all from Gibco).

METHOD DETAILS

NK cell isolation and culture

Single-cell suspensions were obtained by mechanical disruption of spleen tissue, followed by centrifugation and red blood cell lysis using buffered ammonium chloride potassium phosphate solution (ACK buffer). NK cells were isolated using magnetic cell sorting (NK cell isolation kit, mouse, Miltenyi) according to the manufacturer's instructions. NK cells were cultured in either RPMI-1640 (Gibco) or tryptophan-free RPMI-1640 media (Pan Biotech) supplemented with 10% FCS, 1% Penicillin/Streptomycin, 1% L-glutamine, 1% MEM non-essential amino acids, 1 mM sodium pyruvate, 50 μ M β -mercaptoethanol (all from Gibco), and 1700 U/ml of recombinant human IL-2 (NIH). Tryptophan-free media was supplemented with 100 μ M of kynurenine (MedChem express), when indicated. NK cell cultures were maintained under normoxia (20% O₂) or hypoxia (1% O₂). Splenocytes derived from Rag2-deficient mice were resuspended in RPMI-1640 media and incubated at 37°C/5% CO₂ for 2h to remove adherent cells. Non-adherent fraction (enriched in NK cells) was collected and cultured as indicated above.

NK cell stimulation

NK cells were harvested at day 7 of the culture and stimulated for 5h with 1 ng/ml of murine IL-12 (Peprotech) and 20 ng/ml of murine IL-18 (MBL International), or with plate-bound anti-NK1.1 antibody (Biolegend; clone PK136). Golgi Stop™ (BD biosciences) was added to the cells after 1h of stimulation to allow intracellular accumulation of cytokines.

Flow cytometry

Cells were incubated with Fc-receptor-blocking reagent (10% supernatant of anti-CD16/CD32-producing hybridoma 2.4G2) for 15 minutes at 4°C, followed by incubation with fluorochrome-labelled monoclonal antibodies. For the intracellular staining, cells were incubated with Fixation/Permeabilization solution (ThermoFisher Scientific) for 1h at 4°C in the dark. Fluorochrome-labelled monoclonal antibodies against intracellular antigens were incubated with the cells in permeabilization buffer (ThermoFisher Scientific). Apoptotic cells were excluded by labelling with ZombieAqua™ reagent (Biolegend), according to the manufacturer's instructions. For the detection of phosphorylated proteins, cells were sequentially incubated with the Cytofix/Cytoperm™ buffer (BD Biosciences) for 10 min at 37°C, Phosflow Perm buffer III™ for 30 min at 4°C, followed by Fc-receptor-blocking reagent and antibodies. Flow-cytometry was conducted with LSRFortessa™ X-20 flow cytometer (BD Biosciences).

Assessment of NK cell cytotoxicity

NK cells were harvested at day 7 of the culture and then cultured with Cell-Trace™ violet-labelled (5 μ M) tumor cells at a 1:1 ratio for 5h. To detect activation of caspase 3/7, FLICA™ reagent for the detection of caspase activity (Thermo Fisher Scientific) was added for the last hour of the co-culture. Cells were collected and analysed by flow cytometry.

Analysis of NK cell metabolism

NK cells were collected and resuspended in non-buffered, phenol red-free RPMI media (pH 7.4) with glucose (10mM, Agilent), L-glutamine (2mM, Gibco), and sodium pyruvate (1 mM, Agilent). Cells were added into poly-L-lysine-coated plates (XF PDL HS Miniplate, Agilent). Extracellular flux analysis of oxygen consumption and extracellular acidification were performed using HS Mini Analyzer (Agilent). During assay, cells were sequentially treated with 10 μ M oligomycin, 20 μ M carbonyl cyanide-p-trifluoromethoxyphenylhydrazone (FCCP), and combination of 10 μ M rotenone and 10 μ M antimycin A (all from Agilent).

RNA isolation, sequencing and data analysis

NK cells were harvested after 7 days of culture. Cells were lysed and RNA extraction was carried out using the RNeasy® Mini Kit (Qiagen). Concentration of isolated RNA was determined by the Qubit™ 4 Fluorometer and RNA High Sensitivity (HS) kit (Invitrogen). RNA quality was analysed by 2100 Bioanalyzer utilizing RNA 6000 Nano Kit (Agilent). RNA samples of RIN/RQN \geq 9.2 were sequenced by BGI (<https://www.bgi.com/global>).

The raw data were processed using R (version 4.4.2) and bioconductor (version 3.20) in Rstudio (version 2025.04.0). Quality control of clean sequencing reads was performed using FastQC (Babraham Bioinformatics). Low-quality reads were removed using trim_galore (version 0.6.4). The resulting reads were aligned to the mouse genome version GRCm39, and counted using kallisto version 0.46.1.¹¹⁶ The count data was transformed to log₂-counts per million (logCPM) using the voom-function from the limma package.¹¹⁷

Differential expression analysis was performed using the limma package version 3.62.1 in R. A false positive rate of $\alpha = 0.05$ with the false discovery rate (FDR) correction was taken as the level of significance. Volcano plots, heatmaps and Venn diagrams were generated using Enhanced Volcano package (version 1.20.0), the pheatmap package (version 1.0.12), and the browser version of the VennDetail package, respectively. The heatmaps show Z-score-scaled normalized counts of differentially abundant transcripts (Fold change > |1.25|, adjusted p -value < 0.05). The pathway analysis was executed with fgsea package, version 1.32.2. Dot plots were generated using ggplot2 package (version 3.5.1). Transcription factor activity inference was performed using R package DecoupleR (version 2.9.7).⁴³

The genesets were obtained from the geneset package version 0.2.7 using pathway information from KEGG,¹¹⁹ Reactome¹²⁰ and Gene Ontology Consortium.¹²¹ All the gene signatures used in this study are provided in the Table S1.

To define HIF-1 α and AhR regulatory modules (Figure 6), we selected all transcripts with the statistically significant abundance (Fold change > |1.25|, adjusted p -value < 0.05) in at least one of the comparisons between gene-deficient mice and their respective controls. For each transcript, the normalized counts have been z-scored, and the average z-score has been calculated. Mean z-score was used to define regulatory modules as follows:

HIF-1 α -up: (Ncr1^{iCre}Hif1a^{fl/fl} and Ncr1^{iCre} Hif1a^{fl/fl} Ahr^{fl/fl}) < (Hif1a^{fl/fl} and Hif1a^{fl/fl} Ahr^{fl/fl}).

HIF-1 α -down: (Ncr1^{iCre}Hif1a^{fl/fl} and Ncr1^{iCre} Hif1a^{fl/fl} Ahr^{fl/fl}) > (Hif1a^{fl/fl} and Hif1a^{fl/fl} Ahr^{fl/fl}).

AhR-up: (Ncr1^{iCre}Ahr^{fl/fl} and Ncr1^{iCre} Hif1a^{fl/fl} Ahr^{fl/fl}) < (Ahr^{fl/fl} and Hif1a^{fl/fl} Ahr^{fl/fl}).

AhR-down: (Ncr1^{iCre}Ahr^{fl/fl} and Ncr1^{iCre} Hif1a^{fl/fl} Ahr^{fl/fl}) > (Ahr^{fl/fl} and Hif1a^{fl/fl} Ahr^{fl/fl}).

To define the modules related to IL-12R/18R signaling, z-scored matrix of differentially abundant transcript within the “IL-12R IL-18R NF κ B signaling” pathway (Table S1) was used.

To identify the biological processes affected by the defined modules, over-representation analysis was performed on the 150 most significant transcripts (based on the adjusted p -value deriving from gene-deficient mice and their respective controls comparison) with fgsea package (version 1.32.4), and the mouse MSigDB gene ontology biological process gene set (version v2025.1). Dot plots were generated using ggplot2 package (version 3.5.1).

Analysis of mouse and human single-cell transcriptome data

Single-cell dataset GEO: GSE123534⁸ was analysed and visualized using the Seurat R package (version >4.3.0).¹¹⁸ For quality control, features detected in less than three cells, and cells with more than 7,000 and less than 200 genes with non-zero counts, were filtered out. All cells having more than 20% of mitochondrial gene counts or more than 0.5% of haemoglobin counts were excluded. The integration of the samples was performed using Harmony.¹²² Subsequently, the integrated cells were clustered using the umap method. Scores for the gene signatures of interest were calculated using AddModuleScore in seurat.

To analyze the enrichment of our signatures (Table S2) in tumor-infiltrating NK cells of cancer patients, we utilized pan-NK cell cancer atlas⁵³ (<http://pan-nk.cancer-pku.cn>). Multigene geometric means for the signatures were calculated and plotted across the clusters defined in the original publication by Tang et al.⁵³

QUANTIFICATION AND STATISTICAL ANALYSIS

All data were tested for normal distribution using Shapiro-Wilk test, followed by evaluation using an appropriate test and a correction for multiple comparison testing, when necessary (detailed in Figure legends). Data are shown as mean \pm SEM; n denotes the number of independently performed experiments. Organs from individual animals were pooled before cell isolation, culture, and analysis, unless indicated otherwise. Experimental groups were considered significantly different when *, $p \leq 0.05$, **, $p \leq 0.01$, ***, $p \leq 0.001$ and ****, $p \leq 0.0001$. Analysis of sequencing-derived data was detailed in STAR Methods section.